UNIVERSIDAD DE CHILE
FACULTAD DE CIENCIAS FÍSICAS Y MATEMÁTICAS
DEPARTAMENTO DE INGENIERÍA ELÉCTRICA

PERFORMANCE ENHANCEMENT OF OFDM-BASED SYSTEMS USING NYQUIST-I PULSES

MEMORIA PARA OPTAR AL TÍTULO DE INGENIERO CIVIL ELÉCTRICO

HERNÁN FELIPE ARRAÑO SCHARAGER

PROFESOR GUÍA:
DR. CESAR AZURDIA MEZA

MIEMBROS DE LA COMISIÓN:
DR. CLAUDIO ESTÉVEZ MONTERO
DR. JORGE SILVA SÁNCHEZ

SANTIAGO DE CHILE
2015

RESUMEN DE LA MEMORIA PARA OPTAR AL
TÍTULO DE INGENIERO CIVIL ELÉCTRICO
POR: HERNÁN FELIPE ARRAÑO SCHARAGER
FECHA: SEPTIEMBRE 2015
PROFESOR GUÍA: DR. CESAR AZURDIA MEZA

PERFORMANCE ENHANCEMENT OF OFDM-BASED SYSTEMS USING NYQUIST-I PULSES

Los constantes y cada vez más acelerados avances tecnológicos, han generado que los sistemas de comunicación se optimicen considerablemente con el transcurso de los años. Dentro de los cambios más importantes que se han visto en el último tiempo, destaca la disminución del uso de los clásicos sistemas de telecomunicaciones basados en portadoras únicas, dándose paso a sistemas más complejos en donde la información se transmite utilizando múltiples portadoras. Dentro de este último grupo de técnicas, uno de los que más sobresale es *orthogonal frequency division multiplexing* (OFDM), el cual ha sido y es, ampliamente utilizado en múltiples aplicaciones o estándares de comunicación. El uso extensivo de OFDM se debe a varias ventajas que esta técnica posee, tales como: alcanzar altas tasas de transmisión de datos, generar señales robustas ante canales inalámbricos, tener una alta eficiencia espectral, entre otros. Pero, aun cuando éstos exhiben múltiples ventajas, también presentan ciertos inconvenientes que deben ser tratados como lo son: los altos niveles de *peak-to-average power ratio* (PAPR) que caracterizan a las señales OFDM y la sensibilidad a errores originados por la desincronización entre el transmisor y receptor. Esto último, facilita la generación de interferencia entre portadoras (*inter-carrier interference*, ICI) y, por ende, un aumento en la probabilidad de error.

En este trabajo se examina el funcionamiento de los sistemas basados en OFDM, partiendo desde la generación de la señal, hasta su comportamiento espectral. Pero por otro lado, también se analiza como la implementación de pulsos que cumplen con el primer criterio de Nyquist (Nyquist-I), favorece al rendimiento de esta clase de sistemas. El uso de pulsos Nyquist-I para combatir los inconvenientes típicos mostrados por los sistemas basados en OFDM ha sido propuesto por múltiples investigadores. En este trabajo se estudia en detalle una nueva familia de pulsos Nyquist-I llamada *improved parametric linear combination pulses* (IPLCP), la cual se propone para combatir un completo listado de aspectos perjudiciales mostrados por sistemas OFDM reales, a diferencia de otros pulsos que solamente buscan solucionar uno de ellos. Para analizar el rendimiento de la nueva familia de pulsos, se le compara con otras ya conocidas en términos del ICI, la razón señal a interferencia (*signal-to-interference ratio*, SIR), el PAPR y la tasa de probabilidad de error de bit (*bit error rate*, BER). Finalmente, el análisis demuestra que la nueva familia es la que mejor se desempeña en promedio en términos de los parámetros de estudio recién mencionados, dejando en claro que la implementación del IPLCP favorece al rendimiento de los sistemas de comunicación basados en la tecnología OFDM.

Summary

Constant and increasingly rapid technological advances have generated communication systems to be considerably optimized over the past years. Among one of the most important changes that have been seen in recent times, is the fact that the use of classic single carrier communication systems has declined, giving way to more complex systems in which information is transmitted using multiple carriers. Within this latter group of techniques one that stands out is orthogonal frequency division multiplexing (OFDM), which has been widely used in many applications and communication standards. The extensive use of OFDM is due to several advantages that it exhibits, such as achieving high data transmission rates, generating robust signals to deal with typical wireless channels, high spectral efficiency, among others. But even when they show many advantages, there also certain drawbacks that must be addressed, such as the high levels of peak-to-average power ratio (PAPR) that characterize OFDM signals, or the sensitivity to errors caused by desynchronization between the transmitter and receiver. This latter fact facilitates the generation of inter-carrier interference (ICI) and thereby, increases the probability of errors.

In this work the behavior of OFDM-based systems is analyzed in detail, including the generation of the signal and its spectral behavior. But also, we analyze how the implementation of pulses that meet Nyquist's first criterion (Nyquist-I) enhance the performance of such systems. The use of Nyquist-I pulses to address impairments exhibited by OFDM-based systems has been proposed by many scholars. In this work a new family of Nyquist-I pulses called improved parametric linear combination pulses (IPLCP) is studied. This family of pulses aims to combat a list of harmful aspects shown by real OFDM systems, instead of addressing only one of them as mostly every other pulse do. The IPLCP is compared with other well-known pulses to examine the performance of it in terms of the ICI power, the signal-to-interference ratio (SIR) power, the PAPR and the bit error rate (BER). Finally, the analysis shows that the new family of pulses performs well in terms of the recently mentioned parameters, concluding that the implementation of the IPLCP favors the performance of the communication system based on OFDM technology.

A mis padres Jeannette y Hernán.

Acknowledgements

Me mantengo incrédulo ante el hecho de saber que ha llegado este momento. Distantes parecen escucharse esas frases: *"cuando salga de la Universidad..., cuando me titule..., cuando sea Ingeniero..."*. Que rápido parece pasar el tiempo, como si una etapa se cerrara de un instante a otro, para dar paso a una nueva. Pero este camino no lo he recorrido solo, sino que han sido varias las personas que me han acompañado y formado, haciéndome ser quien soy hoy. Me gustaría partir agradeciendo a dos personas que marcan un antes y un después en mis intereses académicos: mis tíos, Magdalena Couve y Horacio Garnham. Gracias por haberme hecho "ver la luz". De no ser por ustedes probablemente estaría estudiando alguna otra carrera.

Quisiera continuar agradeciendo al Profesor Cesar Azurdia, quien me abrió las puertas hacia el mundo de las telecomunicaciones y la investigación internacional. Gracias por ser un verdadero guía y por confiar siempre en mí. También reconocer al Profesor Claudio Estévez, por su ayuda y partidos de tennis compartidos. Al Profesor Jorge Silva, por haberme permitido ser parte de su laboratorio durante estos últimos años, estando siempre dispuesto a aconsejarme. Así también, darle las gracias a José Jullian y toda la gente de DYMEQ, quienes me entregaron valiosísimas enseñanzas.

A mis amigos y partners de estudio durante Plan Común: Matías Aedo, Ignacio Ardiles, Andrés Astudillo, Luis Rodríguez y Gonzalo Rojo. Los dos primeros años de mi carrera universitaria se los debo a ustedes. A mis amigos dentro del Departamento de Ingeniería Eléctrica: Felipe Barrera, Diego Bastias, Nicolás Cifuentes, Angelo Falchetti, Felipe Valle, Tomás Villanueva, y a todo el equipo del *IDS Lab*. Guardo con mucho cariño todos los momentos que compartimos: todos los trabajos, trasnochadas, almuerzos y, por las contadas con los dedos, pero muy recordadas salidas que tuvimos.

Quisiera agradecer a toda mi familia, por respetar mi pasión por la investigación y el trabajo. A mis hermanas Daniela, Javiera y Josefa, quienes han sido desde siempre mis compañeras, amigas y fieles soportes. A mis abuelos, por su inmenso afecto en cada uno de mis pasos. A mi polola Fernanda, quien ha sido "mi cable a tierra" y me ha aguantado todo este tiempo. Gracias por tu cariño, paciencia y constante apoyo. Y finalmente, a quienes va dedicado este trabajo: a mis padres, Jeannette y Hernán. Gracias a ustedes estoy donde estoy, yo simplemente fui tomando y aprovechando las oportunidades que me dieron. Me han escuchado, me han alentado en cada una de mis locuras y, por sobre todo, me han querido incondicionalmente a lo largo de toda mi vida.

Contents

List of Tables

List of Figures

Chapter 1

Introduction

1.1 General Background

During the last years, the ways in which we communicate have been continuously evolving, mainly because the increasingly faster technological progress has led to abruptly change the forms of sharing data approximately every ten years, or less. On the one hand, the invention of cellular technology generated a huge paradigm shift in society, because it gave us the ability to call people instead of places. On the other hand, between each technological shift the transmission rates continue to rise seemingly without limits.

In the 80s, first generation (1G) analog cellular systems allowed users only to make simple phone calls, but at the same time gave them the mobility that society previously could not find in the existing public switched telephone network (PSTN). In the 90s, telecommunication systems were digitized and second generation (2G) networks allowed people to start sharing binary data from their mobile phones. So at this point, users were able to send text messages using the Global System for Mobile Communications (GSM) technology, and in later versions of this technology they were able to establish Internet connections [1], but at browsing speeds that could not be compared to those obtained in present times.

Then, in the year 2000 with the birth of third generation (3G) networks, transmission rates and processing capabilities of data increased significantly, allowing the creation of new mobile applications that facilitated users to access multimedia services, such as downloading music or videos. This last fact led to the use of Internet as a daily practice within the services offered by mobile devices, changing the way of using cellular phones by turning them into the well-known *"smart phones"*, capable of being connected to the network anytime and anywhere.

Currently, fourth generation (4G) networks offer users browsing speeds that are comparable, or superior, to those provided by Wireless Fidelity (WiFi) services at home. Moreover, mobile devices are no longer simple "*smart phones*" but somehow they are increasingly coming to resemble portable computers due to their extraordinary data processing ability. It is for these previous reasons that today users can make video calls or watch streaming media

from their devices without experiencing significant delays. This is why we might say that nowadays mobile devices and networks are not simply used to satisfy the need to talk, but browsing through them has turned into a new way of communication.

Second and third generation technologies were based on code division multiple access (CDMA) technology. The use of orthogonal signals and signal-spreading techniques allowed these kind of systems to almost perfectly address the problem of multiple access, providing a comparative advantage over other technologies. But the lack of scalability into higher data transmission rates that pure CDMA-based systems showed, was a big problem in a world that increasingly demands higher processing capability and transmission rates. This last fact led the standardization groups to juggle the idea of using new techniques for future technological generations. Finally upon the candidates, the winner was not the well-known CDMA, but orthogonal frequency division multiplexing (OFDM).

OFDM is a bandwidth-efficient communication technique that was proposed as a mathematical model in the 60s, but taken into reality in the 90s thanks to technological progress that allowed to generate the discrete Fourier transform (DFT) in digital circuits. Since then, OFDM-based systems have been widely used and adopted by many wireless communications standards, such as Long-Term Evolution (LTE) Advanced, WiFi, Wireless Personal Area Network (WPAN), Worldwide Interoperability for Microwave Access (WiMAX) and terrestrial Digital Video Broadcasting (DVB-T) [2–6]. Further, OFDM-based systems combined with multiple-input multiple-output (MIMO) techniques are being suggested and proposed as key technologies to be implemented at the physical layer of fifth generation (5G) systems and cellular networks [7–10].

The extensive use of OFDM-based systems is due to various advantages, such as low bit error rate (BER) levels, high data rate transmission capability, robustness to multi-path fading given by the ability to convert a frequency selective fading channel into several nearly flat fading channels, high bandwidth efficiency, and by the way OFDM-based systems deal with delay spreads by using guard intervals or cyclic prefixes (CP) [2, 3]. But despite all of the benefits offered by these kind of systems, there are certain technical issues that need to be addressed. OFDM-based systems are characterized by having high peak-to-average power ratio (PAPR) values. Further, they are very sensitive to Doppler spread, distortions within the channel and frequency offset errors caused by the desynchronization between local oscillators in the transmitter and receiver [2, 3, 11, 12]. Furthermore, carrier frequency offset also causes some other impairments, such as attenuation or rotation of subcarriers and inter-carrier interference (ICI) between them. All of these previously mentioned drawbacks increase the error probability rate of the OFDM-based systems, affecting on the reliability and implementation of them.

1.2 Specific Background

High ICI levels in multicarrier communication systems are strongly related with poor BER performances, mainly because interference between carriers generate losses of valuable information unable to be corrected by error correcting codes. Moreover, the disturbance generated

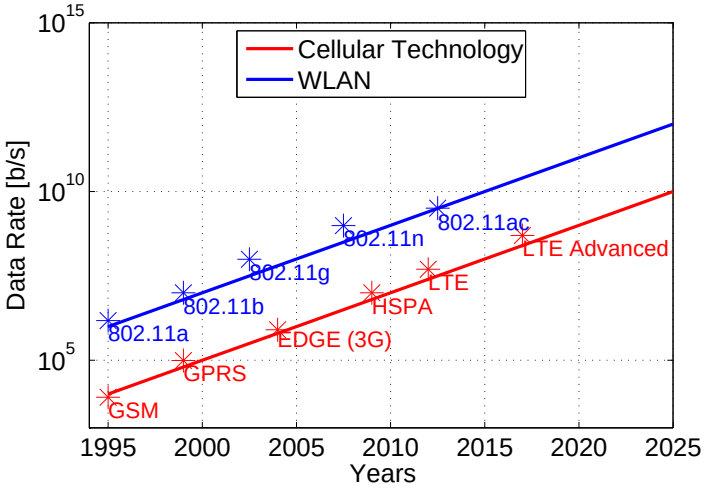

Figure 1.1: Data rate trend for Cellular and WLAN technologies.

by crosstalk may not only affect an specific communication link, but also others, further worsening the situation. Therefore, various methods have been developed to reduce the sensitivity to frequency offset in OFDM-based systems, including windowing at the receiver side, pilot insertion, frequency domain equalization, and ICI self-cancellation schemes [2, 3, 5, 13].

Furthermore, due to the fact that OFDM-based systems exhibit higher PAPR values than prior standards, such as CDMA, Wideband CDMA (WCDMA) or Enhanced Data rates for GSM Evolution (EDGE) [19, 20], the performance of power amplifiers in mobile terminals has to accommodate to operate inside its linear region to guarantee that the transmitted signal will not be distorted [19, 21–23]. Thus, forcing the implementation of an extremely accurate and therefore, more expensive power amplifier to prevent the growth of the BER of the system caused by probable distortions of the signal. In addition, precise digital-to-analog (DAC) and analog-to-digital (ADC) converters have to be used at the transmitter and receiver side respectively, due to greater signal amplitudes produced by high PAPR levels. The latter fact increases even more the cost of the OFDM-based system. As a result, PAPR plays a fundamental role in the design of wireless communication systems. Current ongoing research has focused on the design of new power amplifiers, such as Doherty amplifiers [19, 20, 24] that maintain high efficiency for signals with high PAPR, but unfortunately these technologies are at an experimental stage at the moment.

The need to effectively deal with these two latter impairments shown by OFDM-based systems (ICI and PAPR), led several scholars to propose, study and implement Nyquist-I pulses as a novel solution to them. Pulses such as the raised cosine (RC) pulse, 'better than' raised cosine (BTRC) pulse [14], sinc power (SP) pulse [15], improved sinc power (ISP) pulse [16], new windowing function (NW) [17], and the phase modified sinc pulse (PM) [18] are some of the best-known pulses among a vast list. At the moment, each pulse focuses in solving different OFDM-based systems issues separately, e.g. the BTRC for reducing the ICI, even though the ISP and NW are probably at the moment the ones that best diminish the effects of frequency offsets, the PM accurately minimizes the BER, and so on. But non of them exhibits an all-around performance, i.e. there is no such pulse designed to address each and every drawback exhibited by the system simultaneously. Therefore, as new technical

challenges appear, or as error-free communication links and higher data rates are eventually going to be demanded in next generation networks, as seen in Fig. 1.1, the design and implementation of new families of Nyquist-I pulses will become a fundamental research topic in the upcoming years.

1.3 Overall Objective

In this work a new family of Nyquist-I pulses called the improved parametric linear combination pulse (IPLCP) is studied and proposed. The main objective of the work is to evaluate its efficiency in OFDM-based systems by using theoretical and numerical simulations, proving that the proposed pulse addresses well the most common issues exhibited by these kind of systems.

1.4 Specific Objectives

- Comprehend Nyquist's first criterion for distortionless transmission and understand how it may be useful for analyzing OFDM multicarrier transmission schemes.
- Understand how an OFDM-based system works and how channel distortions or devices impairments may damage the transmitted signal.
- Simulate real OFDM-based system scenarios to validate theoretical results.
- Show that the IPLCP performs well in OFDM-based systems when compared to other existing pulses in terms of the ICI power, signal-to-interference ratio (SIR) power, PAPR and BER.

1.5 Structure of the Thesis

This work has the following organization:

- Chapter 2 presents Nyquist's first criterion for distortionless transmission.
- Chapter 3 introduces the OFDM-based system model and the main impairments that they exhibit. At the same time, it examines the different families of Nyquist-I pulses already proposed by other scholars and introduces the IPLCP.
- Chapter 4 analyses the performance of the IPLCP pulse by using theoretical expressions and by implementing a real OFDM-based system via numerical simulations. The performance of the IPLCP is evaluated in terms of the ICI power, SIR power, PAPR, and BER.
- Chapter 5 presents the conclusions and possible future work.

Chapter 2

Nyquist's Criteria

Obtaining favorable conditions for distortionless transmission links is a fundamental topic in communication systems. In [25], Harry Nyquist established three well-known criteria for achieving the desired non-interfering feature. This chapter studies Nyquist's first criterion and from it derives the notion of Nyquist-I pulses.

2.1 Band-Limited AWGN Channels

The main goal of almost every communication system is to effectively send information from a given source into a receiver over a certain communication channel. When talking about digital systems, the information transmitted is represented by binary data or bits. These information bits are derived from the information source and mapped into analog signals to further being transmitted over the channel in a process called digital modulation. The receiver's aim is to detect the received signal and determine the original bit sequence sent by the transmitter. The baseband transmitted signal for any type of digital modulation scheme may be written as follows,

$$d(t) = \sum_{k=0}^{\infty} I_k g(t - kT) \tag{2.1}$$

where $\{I_k\}$ is a discrete information sequence, T is the bit period (signal period) and $g(t)$ is a pulse-shaping function.

Further, lets suppose that the channel in which the signal travels adds additive white Gaussian noise (AWNG) and also that it is bandlimited to some specified bandwidth, W. Under these conditions, the channel may be considered as a lowpass filter in which the frequency response of the channel, written as $C(f)$, is zero for every out-of-band frequency ($|f| > W$). Therefore the received signal at the receiver side can be represented as

$$r(t) = \sum_{k=0}^{\infty} I_k h(t - kT) + n(t), \tag{2.2}$$

where $n(t)$ represents the AWGN contribution in the signal and

$$h(t) = \int_{-\infty}^{\infty} c(\tau) g(t-\tau) d\tau \tag{2.3}$$

is the convolution between the impulse response of the channel, $c(t)$, and the pulse-shaping function.

Furthermore, lets suppose that a "*match-filter*" is implemented on the receiver side to maximize the signal-to-noise ratio (SNR), then the output of the receiving filter may be given as

$$y(t) = \sum_{k=0}^{\infty} I_k x(t-kT) + \tilde{n}(t), \tag{2.4}$$

where $x(t)$ is a pulse-shaping function that represents the response of the receiving filter to the input pulse $h(t)$, and $\tilde{n}(t)$ is the response of the receiving filter to noise contribution $n(t)$.

Given a bit rate $R = 1/T$, and supposing that $y(t)$ is sampled at instants $t = mT + \tau_{\text{trans}}$, where $m \in \{0, 1, 2, \ldots\}$ and τ_{trans} represents the transmission delay, which is defined as

$$\tau_{\text{trans}} = \frac{\text{data length}}{R}. \tag{2.5}$$

Then (2.4) can be expressed as [26]

$$y(mT + \tau_{\text{trans}}) \equiv y_m = \sum_{k=0}^{\infty} I_k x(mT - kT + \tau_{\text{trans}}) + \tilde{n}(mT + \tau_{\text{trans}}), \tag{2.6}$$

$$y_m = I_m + \sum_{\substack{k=0 \\ k \neq m}}^{\infty} I_k x_{m-k} + \tilde{n}_m. \tag{2.7}$$

In (2.7), I_m is the desired information at the m-th sampling instant, whereas the term

$$\sum_{\substack{k=0 \\ k \neq m}}^{\infty} I_k x_{m-k} \tag{2.8}$$

represents the inter-symbol interference (ISI) factor, and $\tilde{n}_m$ is the contribution of the noise at the m-th sampling instant.

2.2 Nyquist's First Criterion

Lets suppose that the transmission link is carried over an ideal bandlimited frequency-flat channel. Therefore, its frequency response may be written as

$$C(f) = \begin{cases} 1, & \text{if } |f| \leq W \\ 0, & \text{if } |f| > W. \end{cases} \tag{2.9}$$

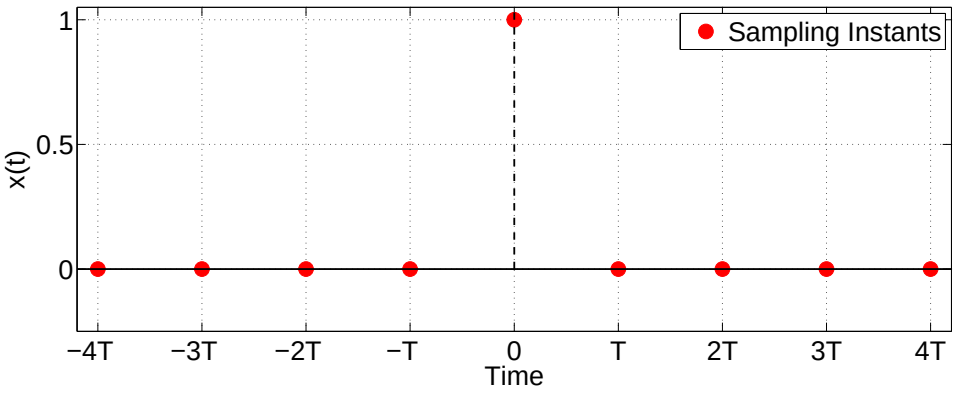

Figure 2.1: Zero ISI condition.

Our goal is to find a pulse $g(t)$, consequently also a function $x(t)$, that result in zero ISI. Given (2.7), the condition for obtaining no contribution from other signal element at the sampling instant is

$$x(mT) \equiv x_m = \begin{cases} 1, & \text{if } m = 0 \\ 0, & \text{if } m \neq 0, \end{cases} \tag{2.10}$$

as represented in Fig. 2.1.

Given the fact that the channel is bandlimited and from the behavior of the pulse in Fig. 2.1, lets try to derive a condition of the Fourier transform of $x(t)$, $X(f)$, in order for $x(t)$ to satisfy (2.10). On the one hand, we known that inverse Fourier transform of $X(f)$ is written as

$$x(t) = \int_{-\infty}^{\infty} X(f) \mathrm{e}^{j2\pi ft} df, \tag{2.11}$$

and at the sampling instants, $t = mT$, (2.11) may be expressed as

$$x(mT) = \int_{-\infty}^{\infty} X(f) \mathrm{e}^{j2\pi fmT} df. \tag{2.12}$$

By dividing the integral in (2.12) into integrals covering the bandwidth of the system, $1/T$, we obtain

$$x(mT) = \sum_{i=-\infty}^{\infty} \int_{(2i-1)/2T}^{(2i+1)/2T} X(f) \mathrm{e}^{j2\pi fmT} df \tag{2.13}$$

$$= \sum_{i=-\infty}^{\infty} \int_{-1/2T}^{1/2T} X\left(f + \frac{i}{T}\right) \mathrm{e}^{j2\pi fmT} df \tag{2.14}$$

$$= \int_{-1/2T}^{1/2T} \left[\sum_{i=-\infty}^{\infty} X\left(f + \frac{i}{T}\right)\right] \mathrm{e}^{j2\pi fmT} df \tag{2.15}$$

$$= \int_{-1/2T}^{1/2T} A(f) \mathrm{e}^{j2\pi fmT} df \tag{2.16}$$

where $A(f)$ is clearly defined as

$$A(f) = \left[\sum_{i=-\infty}^{\infty} X\left(f + \frac{i}{T}\right)\right]. \tag{2.17}$$

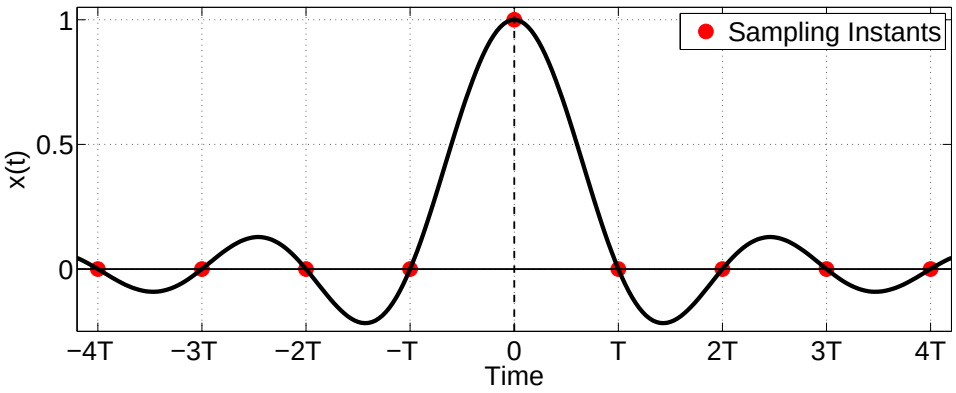

Figure 2.2: Zero ISI sinc function.

From (2.17), we can observe that $A(f)$ behaves as a periodic function with period $1/T$ and therefore, it can be written as the sum of sinusoids, or in other words, it can be expanded in terms of its Fourier series coefficients $\{a_m\}$ as

$$A(f) = \sum_{m=-\infty}^{\infty} a_m \mathrm{e}^{j2\pi mfT}, \tag{2.18}$$

where each coefficient is given by

$$a_m = T \int_{-1/2T}^{1/2T} A(f) \mathrm{e}^{-j2\pi mfT}. \tag{2.19}$$

Further, by analyzing (2.16) and (2.19), we obtain the following

$$a_m = Tx(-mT). \tag{2.20}$$

Therefore, the necessary and sufficient condition for (2.12) to be satisfied is that the Fourier series coefficients behave as

$$a_m = \begin{cases} T, & \text{if } m = 0 \\ 0, & \text{if } m \neq 0, \end{cases} \tag{2.21}$$

which, when replaced into (2.18) returns

$$A(f) = T \tag{2.22}$$

or identically,

$$\sum_{i=-\infty}^{\infty} X\left(f + \frac{i}{T}\right) = T. \tag{2.23}$$

Finally, it is worth mentioning that the expression (2.10) is known as Nyquist's condition for distortionless transmission. And on the other hand, (2.23) represent Nyquist's first criterion (Nyquist-I) for distortionless transmission.

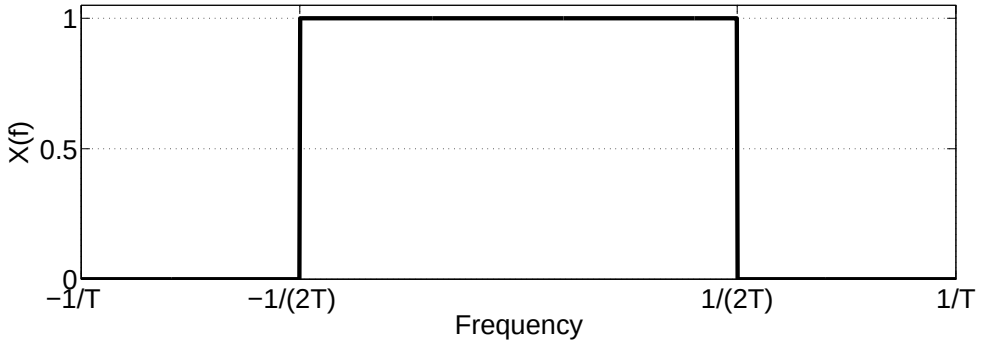

Figure 2.3: Spectrum of the sinc function.

2.2.1 Nyquist-I Pulse

Mathematical functions that satisfy Nyquist's first criterion are often called Nyquist-I pulses. The most straightforward solution to the latter pair of equations that meet the ISI-free property is the sinc function, which may be expressed as

$$x(t) = \text{sinc}(\pi R t) = \frac{\sin(\pi R t)}{\pi R t} = \frac{\sin\left(\frac{\pi}{T}t\right)}{\frac{\pi}{T}t}. \tag{2.24}$$

It is easy to demonstrate that

$$\text{sinc}(\pi R t) = \begin{cases} 1, & \text{if } t = 0 \\ 0, & \text{if } t = \pm T, \pm 2T, \pm 3T, \ldots, \end{cases} \tag{2.25}$$

as seen in Fig. 2.2. Also, this pulse is bandlimited and has a frequency-flat response. Its Fourier transform is given by

$$X(f) = \frac{1}{R}\Pi\left(\frac{f}{R}\right), \tag{2.26}$$

where $\Pi(\cdot)$ represents the rectangular function. Moreover, the frequency behavior of the sinc pulse and the representation of multiple sinc functions transmitted over a certain interval of time are shown in Figure 2.3 and 2.4, respectively.

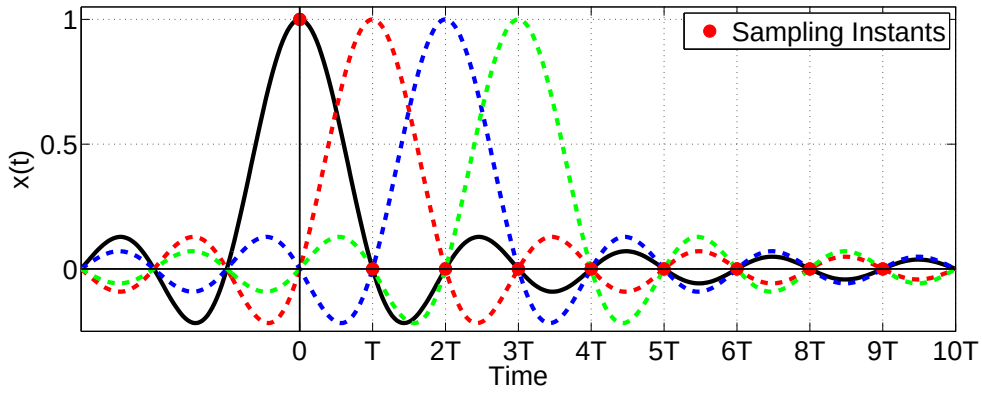

Figure 2.4: Multiple sinc pulses transmitted over a time interval.

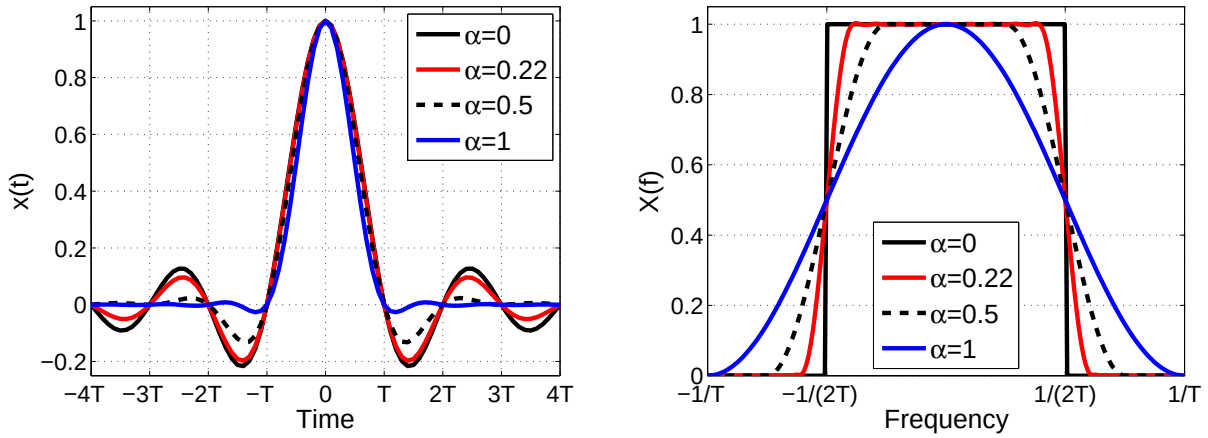

(a) (b)

Figure 2.5: (a) and (b) show the time and frequency-domain behavior, respectively, of the raised cosine pulse for different values of α.

Unfortunately, even though the latter pulse is the one that possesses the minimum bandwidth and that satisfies the zero ISI property at the sampling instants, it has a slow decay rate of $1/t$ [27]. Further, it has infinite support in the time domain and it is non-causal, therefore nonrealizable.

By increasing the width of the spectrum, in order to make the pulse sidelobes (tails) to decay more rapidly, we can define a pulse with bandwidth

$$W' = \frac{1}{2}(1+\alpha)R, \tag{2.27}$$

where α is defined as the *roll-off factor* and may take any real value between 0 and 1. In simple terms, the parameter α represents the excess bandwidth occupied by the signal beyond the sampling frequency boundary. A particular pulse spectrum that satisfies the relation stated in (2.27) is the raised cosine. This latter pulse-shaping function is widely used in baseband modulation schemes and filtering techniques [28]. Its time-domain expression is given by,

$$x_{RC}(t) = \operatorname{sinc}(\pi R t)\frac{\cos(\pi\alpha R t)}{1-(2\alpha R t)^2} \tag{2.28}$$

$$= \operatorname{sinc}\left(\pi\frac{t}{T}\right)\frac{\cos\left(\pi\alpha\frac{t}{T}\right)}{1-\left(2\alpha\frac{t}{T}\right)^2}, \tag{2.29}$$

which has a decay rate of $1/t^3$ for values of $\alpha > 0$ [26]. In addition, its frequency-domain

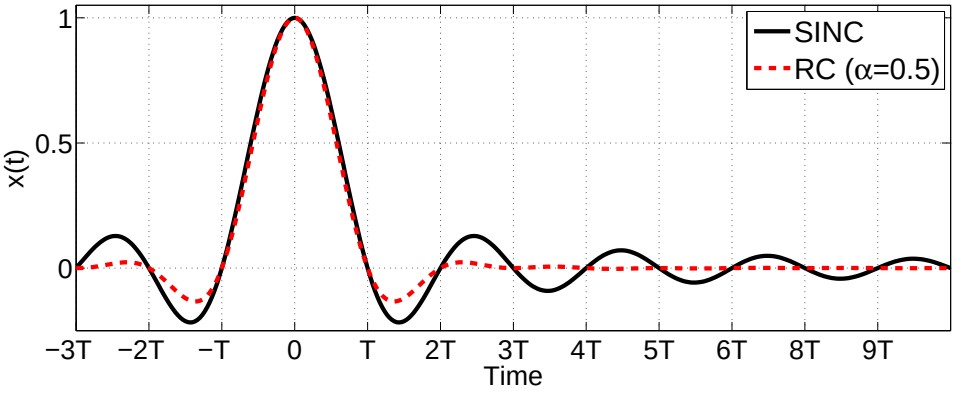

Figure 2.6: Comparison of the sinc function and raised cosine pulse.

spectrum behaves as follows [28],

$$X_{RC}(f) = \begin{cases} T, & \text{if } |f| \leq \dfrac{1-\alpha}{2T} \\ T\cos^2\left(\dfrac{\pi T}{2\alpha}\left(|f| - \dfrac{1-\alpha}{2T}\right)\right), & \text{if } \dfrac{1-\alpha}{2T} \leq |f| \leq \dfrac{1+\alpha}{2T} \\ 0, & \text{if } |f| > \dfrac{1+\alpha}{2T}. \end{cases} \tag{2.30}$$

It is possible to notice that the time-domain expression of the raised cosine pulse is equal to the sinc function for $\alpha = 0$. Further, by plotting the time and frequency-domain behavior of the raised cosine pulse, as seen in Fig. 2.5, one may notice that for greater values of α the time-domain sidelobes decay faster, but in expenses of a wider bandwidth occupied by the signal. This latter time-domain characteristic enables baseband communication systems to use pulses with small sidelobes amplitudes, to effectively minimize the ISI that arises due to channel impairments or external signal sources. Thus, helping the system's BER level to be maintained, even though the conditions offered by the link are not the most favourable. A comparison of the sinc and raised cosine pulse for $\alpha = 0.5$, can be seen in Fig. 2.6.

2.3 Summary and Final Remarks

This part of the work provides expressions that characterize the transmission of information over typical baseband digital modulation schemes. Also, the mathematical definition of the inter-symbol interference was derived. In addition, Nyquist's first criterion for distortionless transmission over AWGN channels was studied and with it, the minimum bandwidth pulse that satisfies the ISI-free property was obtained. However, it was shown that the tails of this minimum bandwidth pulse decay as $1/t$, fact that could be problematic for practical filter design and for symbol timing recovery. Due to this and other disadvantages that the sinc function exhibit, another pulse-shaping function with an increased bandwidth characteristic

was introduced, improving the time-domain dacay rate, but damaging the spectrum behavior as it occupies an excess bandwidth.

As it will be shown later, the use of Nyquist-I pulses is not restricted to time-domain expressions, digital modulation schemes or ISI-free purposes. But its sinusoidal behavior could also be useful in the frequency-domain as the number of applications using orthogonal signals increases and the need for better spectral management becomes a key factor in nowadays communication systems.

Chapter 3

OFDM-Based System Model and Nyquist-I Pulses

3.1 Introduction and Block Diagram

As previously indicated, OFDM is a concept that has been built for several years but it became a practical reality when the birth of applications coincided with developments in electronics and new efficient softwares [29]. OFDM is a transmission scheme where a high-rate serial data stream is divided into a set of parallel low-rate substreams. In OFDM, the inverse discrete Fourier transform (IDFT) and Discrete Fourier Transform (DFT) are used for modulating and demodulating each low-rate data symbol on a different orthogonal subcarriers, respectively. In simple words, an OFDM symbol (IDFT output samples) is formed by the sum of N data constellation points $\{d_k\}$ traveling on a subcarrier, where phase-shift keying (PSK), quadrature amplitude modulation (QAM), or other type of digital modulation schemes may be used for the symbol mapping. Further, N is also the number of IDFT/DFT points.

A simple representation of the time-domain complex envelope of an OFDM symbol can be written as [18,30]

$$s(t) = \mathrm{Re}\left\{ \mathrm{e}^{j2\pi f_c t} \sum_{k=0}^{N-1} p(t) d_k \mathrm{e}^{j2\pi f_k t} \right\}, \tag{3.1}$$

where j is the imaginary unit ($\sqrt{-1}$), f_k is the k-th subcarrier frequency, f_c is the central carrier frequency and $p(t)$ is a pulse-shaping function that limits or narrows each data constellation point in a certain interval of time. A simplified scheme of an OFDM-based transceiver is shown in Fig. 3.1.

By analyzing (3.1) and by knowing that in OFDM the original message is divided into smaller low-rate fragments, each traveling on different orthogonal subcarriers, one may notice that the bandwidth of the subcarriers becomes small compared with the coherence bandwidth of the channel. This last feature allows simple equalization and also makes OFDM signals more robust to typical wireless environments, because it converts a frequency selective fading

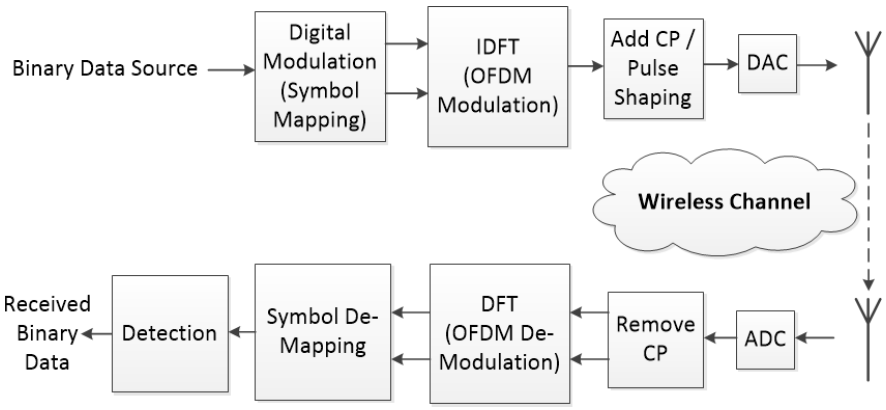

Figure 3.1: General scheme of an OFDM transceiver.

channel, into several nearly flat fading channels, decreasing the losses and error rate at the receiver side.

Furthermore, orthogonal subcarriers allow OFDM-based systems to have better spectral containment and efficiency, because the Fourier transform of the various data overlaps by using the principle of orthogonality, as seen in Fig. 3.2. This latter fact increases the available bandwidth, enabling OFDM-based systems to reach transmission rates much higher than other technologies.

On the other hand, OFDM-based systems generally uses guard intervals or CP, whose lengths exceed the maximum excess delay of the multipath propagation channel. Due to this, systems are able to cancel almost completely the delay spread phenomena at the receiver side. The delay spread effect arises when the receiver gets the same message repeated over time, since the signal takes different paths when irradiated in all directions by the antenna of the transmitter. This latter issue may generate interference or degradation of the signal, and it is a common problem observed in cellular communication systems.

For the system shown in Fig. 3.1 and from (3.1), we assume that the input data symbols are uncorrelated, where $\{d_k\}$ is a zero-mean independent sequence of unit variance and normalized symbol energy, meaning that

$$E[d_k d_m^*] = \begin{cases} 1, & \text{if } k = m \\ 0, & \text{if } k \neq m. \end{cases} \tag{3.2}$$

Also, as mentioned above, one very important characteristic of OFDM-based systems is the fact that subcarriers are orthogonal with one another. To ensure orthogonality the following relationship must be satisfied

$$f_k - f_m = \frac{k-m}{T}, \quad (k,m) \in \{0, 1, \ldots N-1\}, \tag{3.3}$$

where T is the OFDM symbol duration and $1/T$ the minimum required subcarrier frequency spacing to satisfy orthogonality. Therefore, individual subcarrier frequencies can be defined as

$$f_k = \frac{k}{T}, \quad \forall k \in \{0, 1 \ldots N-1\}. \tag{3.4}$$

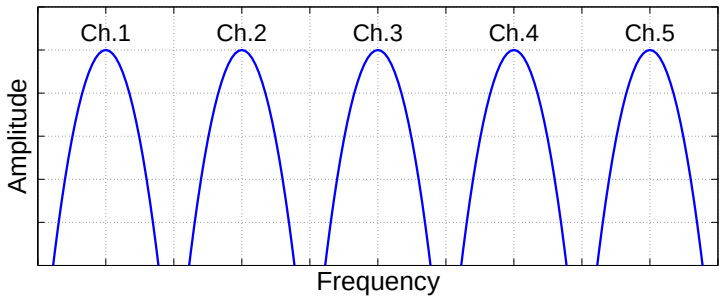

(a) Frequency-division multiplexing (FDM) spectral representation.

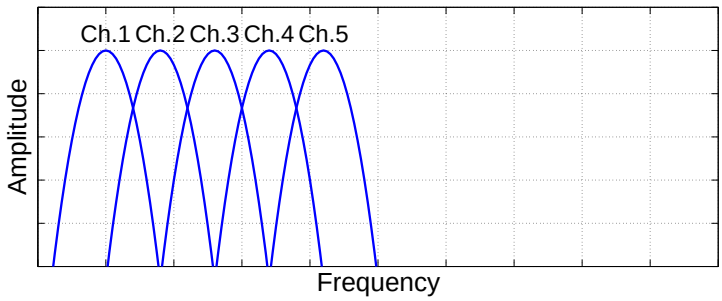

(b) OFDM spectral representation.

Figure 3.2: OFDM spectral efficiency.

From above, one may notice that each subcarrier has exactly an integer number of cycles in the interval T, and the number of cycles between adjacents subcarriers differs by exactly one [3].

3.1.1 OFDM Demodulation

Lets suppose that the OFDM signal in (3.1) travels over an ideal noiseless channel and that it has already been downconverted from its central carrier. The information carried in the m-th subcarrier is demodulated just by downconverting the OFDM symbol by a frequency equal to m/T and then integrating the resulting signal over a interval of time of duration T. Basically, this is making the reverse operation to (3.1), or simply extracting the Fourier coefficients from the received time-domain signal $s(t)$ (equivalent to computing the DFT).

Further and for the sake of simplicity, if one supposes that the pulse-shaping function, $p(t)$, is equal to unity over the symbol period T, the demodulation process may be written as follows,

$$\hat{d}_m = \frac{1}{T}\int_0^T \mathrm{e}^{-j2\pi\left(\frac{m}{T}\right)t}\sum_{k=1}^{N} d_k \mathrm{e}^{j2\pi\left(\frac{k}{T}\right)t}dt \tag{3.5}$$

$$= \frac{1}{T}\sum_{k=1}^{N} d_k \int_0^T \mathrm{e}^{-j2\pi\left(\frac{k-m}{T}\right)t - t_s} \tag{3.6}$$

$$= d_m, \tag{3.7}$$

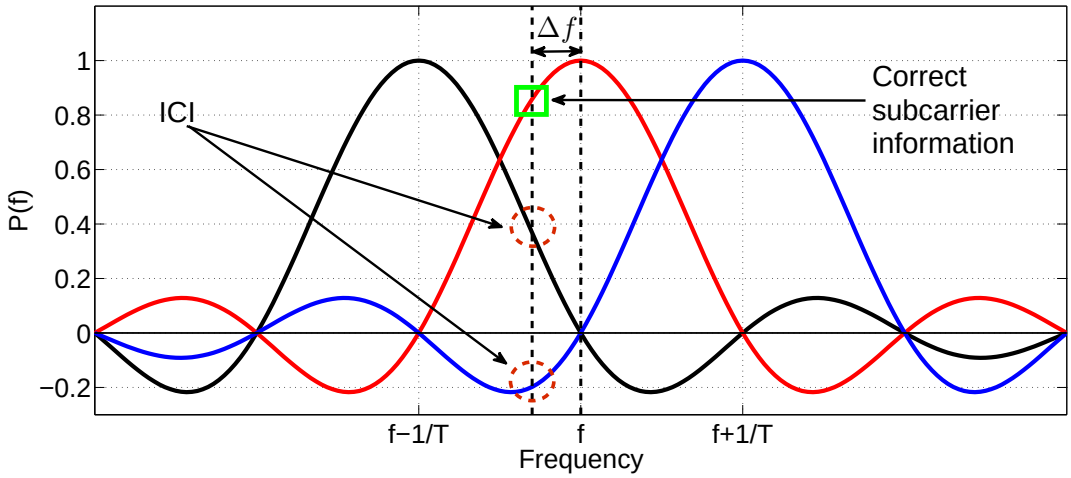

Figure 3.3: Carrier desyncronization generates ICI.

where $\hat{d}_m$ represents the decision variable in the receiver side. So, for the m-th demodulated subcarrier, the integration gives the desired output d_m. Furthermore, it is possible to demonstrate that for all the other subcarriers, the integration in (3.6) is zero, because the frequency difference $(k-m)/T$ produces an integer number of cycles within the interval symbol period, resulting in an integral always equal to zero.

3.2 Carrier Desynchronization

OFDM-based systems are characterized for having some drawbacks compared with common single carrier modulation schemes. Frequency offsets, Δf, phase errors, θ, and noise, n, are introduced due to channel distortion and desynchronization between the crystal oscillator of the transmitter and receiver in these type of systems. These impairments may generate interference within the subcarriers, resulting in valuable data losses and therefore, increasing the BER of the system.

If one adds the listed above errors to $s(t)$ in (3.1), the received downconverted signal ends up being expressed as

$$r(t) = \mathrm{e}^{2\pi(\Delta f)t+\theta} \sum_{k=0}^{N-1} d_k p(t) \mathrm{e}^{j2\pi f_k t} + n(t). \tag{3.8}$$

From Section 3.1.1, the decision variable for the transmitted symbol d_m may be written as

$$\hat{d}_m = \frac{1}{T} \int_0^T r(t) \mathrm{e}^{-j2\pi f_m t} dt, \tag{3.9}$$

which could be decomposed into

$$\hat{d}_m = d_m \mathrm{e}^{j\theta} P\left(-\Delta f\right) + \mathrm{e}^{j\theta} \sum_{\substack{k=0 \\ k\neq m}}^{N-1} d_k P\left(\frac{m-k}{T} - \Delta f\right) + \widetilde{n}(t), \tag{3.10}$$

where $P(f)$ is defined as the Fourier transform of the pulse-shaping function $p(t)$. Furthermore, the power of the desired signal can be calculated as

$$\sigma_m = |d_m|^2 \, |P(\Delta f)|^2 \,, \tag{3.11}$$

and the ICI power is given as follows [31]

$$\sigma_{\text{ICI}}^m = \sum_{\substack{k=0 \\ k\neq m}}^{N-1} \sum_{\substack{n=0 \\ n\neq m}}^{N-1} d_k d_n^* P\left(\frac{k-m}{T} + \Delta f\right) P\left(\frac{n-m}{T} + \Delta f\right). \tag{3.12}$$

Considering (3.2) and (3.12), the average ICI power is written as

$$\text{P}_{\text{ICI}} = \overline{\sigma_{\text{ICI}}^m} = \sum_{\substack{k=0 \\ k\neq m}}^{N-1} \left| P\left(\frac{k-m}{T} + \Delta f\right)\right|^2. \tag{3.13}$$

Notice that the average ICI power mainly depends on the value of the frequency offset, Δf, and the pulse-shaping function spectrum, $P(f)$. The latter fact demonstrate the importance of choosing the right pulse-shaping function for a particular OFDM-based system design. An scheme of how ICI arises due to carrier desynchronization is shown in Fig. 3.3.

Given (3.13), the SIR power expression is derived straightforward, basically because it is defined as the ratio of average signal power, $|P(\Delta f)|^2$, to average ICI power, resulting in

$$\text{SIR} = \frac{|P(\Delta f)|^2}{\sum\limits_{\substack{k=0 \\ k\neq m}}^{N-1} \left| P\left(\frac{k-m}{T} + \Delta f\right)\right|^2}. \tag{3.14}$$

Similarly to the average ICI power, the expression given by (3.14) depends on the frequency offset, Δf, and the pulse-shaping function spectral behavior, $P(f)$, so again its choice plays a important role in the overall performance of the system.

3.3 PAPR Analysis

The PAPR is a dimensionless quantity that measures the ratio of peak values, to mean or effective value for a given signal. The formal PAPR expression for any signal may be written as follows

$$\text{PAPR} = \frac{|s(t)|^2_{\text{peak}}}{s(t)^2_{\text{rms}}} = \frac{\text{peak power}}{\text{average power}}, \tag{3.15}$$

where "rms" stands for the root-mean-square.

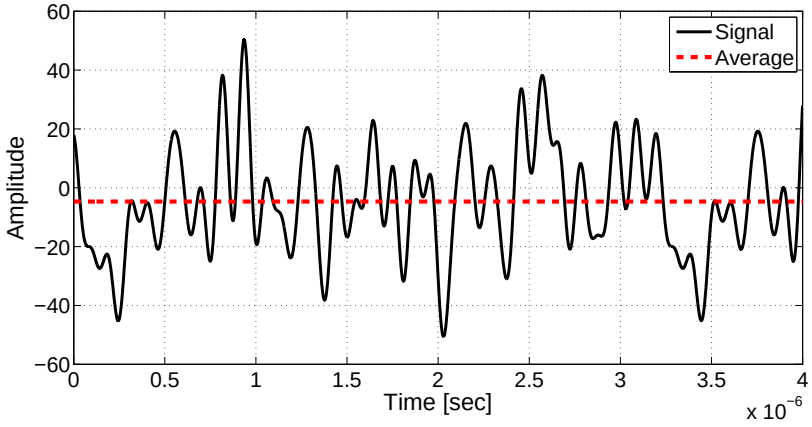

Figure 3.4: OFDM time-domain signal based on IEEE 802.11a specifications.

One of the main characteristics of OFDM-based system signals, is the fact that that they exhibit relative large PAPR values, as seen in Fig. 3.4, where a time-domain signal based on the Institute of Electrical and Electronics Engineers (IEEE) 802.11a (WiFi) protocol has been simulated and plotted. This latter effect tends to reduce the power efficiency of the radio frequency amplifier, increasing the energy consumption in user equipments (UE).

In addition, some probability and statistics tools are useful to analyze the PAPR behavior in communication systems. One of them is detailed below in Section 3.3.1.

3.3.1 Complementary Cumulative Distribution Functions

The cumulative distribution function (CDF), or distribution function F_X of the random variable X, is defined as the probability that the random variable X falls below some particular value x [32]. Mathematically speaking this is,

$$F_X(x) = \mathbb{P}(X \leq x) = \int_{-\infty}^{x} f_X(t)dt, \tag{3.16}$$

for some positive measurable function $f_X : \mathbb{R} \to [0, \infty)$, which is known as the probability density function (PDF). On the other hand, the complementary cumulative distribution function (CCDF) of X is defined to be

$$\tilde{F}(x) = \mathbb{P}(X > x) = 1 - F(x) = \int_{x}^{\infty} f_X(t)dt. \tag{3.17}$$

In signal processing, the CCDF curve shows the amount of time a signal spends above the average power level of the measured signal, or equivalently, the probability that the signal power will be above the average power level. This latter expressions are useful to study the PAPR of an OFDM-based system signal and therefore, they are used in this work for obtaining results from simulations in Chapter 4.

3.4 BER Analysis

Although reducing the ICI and PAPR, and maximizing the SIR is of great benefit for the OFDM-based systems, the BER is probably the most important evaluation metric in the design of an optimal pulse-shaping function [11]. Therefore, the BER plays a fundamental role in assessing the performance and effectiveness of a digital communication system.

3.4.1 The Decision Regions and Error Probability

If we denote $s_m(t)$ as a particular signal $s(t)$ from (3.1) in which data d_m is transmitted, $s_m(t)$ can be represented by a vector $\mathbf{s_m} \in \mathbb{R}^N$. Lets note that the set of subcarriers form itself a set of linearly independent vectors, so it is possible to consider an OFDM-based system as being formed by an orthonormal basis.

Moreover, the received signal, $r(t)$, may also be decomposed into a vector $\mathbf{r} \in \mathbb{R}^N$. The receiver observes the received signal and from it makes an optimal decision about what symbol was transmitted. The optimal decision arises from a decision that minimizes the probability of error between the transmitted message, d_m, and the detected message, $\hat{d_m}$. This error probability is given by

$$P_e = \mathbb{P}\left[\hat{d_m} \neq d_m\right]. \tag{3.18}$$

If each transmitted symbol is formed by b_s bits then

$$M = 2^{b_s}, \tag{3.19}$$

represents the number of possible messages that can be formed. Further, the detector in the receiver side partitions the output space $\mathbb{R}^N$ into M regions denoted by $\mathrm{DR}_1, \mathrm{DR}_2, \ldots, \mathrm{DR}_M$, such that the detector makes the optimal decision in favor of d_m. The region DR_m, is called the decision region for data d_m.

To determine the error probability of a detection scheme, we note that when $\mathbf{s_m}$ is transmitted, an error occurs when the received signal $\mathbf{r}$ is not in DR_m. The symbol error probability of a receiver with decision regions $\{\mathrm{DR}_m \mid 1 \leq m \leq M\}$ is therefore given by

$$P_e = \sum_{m=1}^{M} P_{d_m} \mathbb{P}\left[\mathbf{r} \notin \mathrm{DR}_m \mid d_m \text{ sent}\right] \tag{3.20}$$

where P_{d_m} is the probability of choosing d_m as the transmitting symbol from the set of all M possible messages. Now, for equally likely messages $P_{d_m} = 1/M$,(3.20) may be written

as [33]

$$P_e = \frac{1}{M}\sum_{m=1}^{M}\mathbb{P}\left[\mathbf{r}\notin \mathrm{DR}_m \mid d_m \text{ sent}\right] \tag{3.21}$$

$$= 1-\frac{1}{M}\sum_{m=1}^{M}\mathbb{P}\left[\mathbf{r}\in \mathrm{DR}_m \mid d_m \text{ sent}\right] \tag{3.22}$$

$$= 1-\frac{1}{M}\sum_{m=1}^{M}\int_{\mathrm{DR}_m}\mathbb{P}\left[\mathbf{r}|d_m\right]d\mathbf{r}. \tag{3.23}$$

In this work, to evaluate the BER of the system based on the pulse-shaping function chosen, we use (3.23) and also a theoretical expression derived in [11]. This theoretical expression is used to compare the BER of different pulse-shaping functions over an AWGN channel using binary PSK (BPSK) modulation. The average BER is given as a function of the carrier phase noise, θ, ICI power ($\mathrm{P_{ICI}}$), carrier frequency offset, Δf, and the pulse-shaping function spectrum, $P(f)$. The average BER is given as follows

$$\mathrm{BER_{OFDM}} = 1-(1-\mathrm{OFDM_{symbol}})^N, \tag{3.24}$$

where N represents the number of subcarriers or symbols per modulated block. Further, the BER of an OFDM-BPSK communication system sysmbol may be expresses as

$$\begin{aligned}\mathrm{BER_{symbol}} = \frac{1}{2}\Big(&Q\left\{\cos\theta\left[P\left(-\Delta f\right)+\sqrt{P_{ICI}}\right]\sqrt{2\gamma_b}\right\}\\ &+Q\left\{\cos\theta\left[P\left(-\Delta f\right)-\sqrt{P_{ICI}}\right]\sqrt{2\gamma_b}\right\}\Big),\end{aligned} \tag{3.25}$$

where $\gamma_b = E_b/N_0$ is the SNR per bit, being E_b the bit energy, N_0 the noise spectral density and the function $Q(\cdot)$ is defined as,

$$Q(t) = \frac{1}{\sqrt{2\pi}}\int_t^{+\infty}\mathsf{e}^{-x^2/2}dx. \tag{3.26}$$

If the spectral sidelobes of the pulse-shaping functions are very small in comparison to its main lobe, meaning that

$$P(-\Delta f) \gg \mathrm{P_{ICI}} = \sum_{\substack{k=0\\k\neq m}}^{N-1}\left|P\left(\frac{k-m}{T}+\Delta f\right)\right|^2, \tag{3.27}$$

then (3.25) can be approximated to the following expression

$$\mathrm{BER_{symbol}} \approx Q\left[\cos\left(\theta\right)P\left(-\Delta f\right)\sqrt{2\gamma_b}\right]. \tag{3.28}$$

As it is further analyzed in Fig 3.8, for every pulse-shaping function (3.27) is satisfied, therefore in this work we will evaluate the BER of the proposed system using the expression given in (3.28).

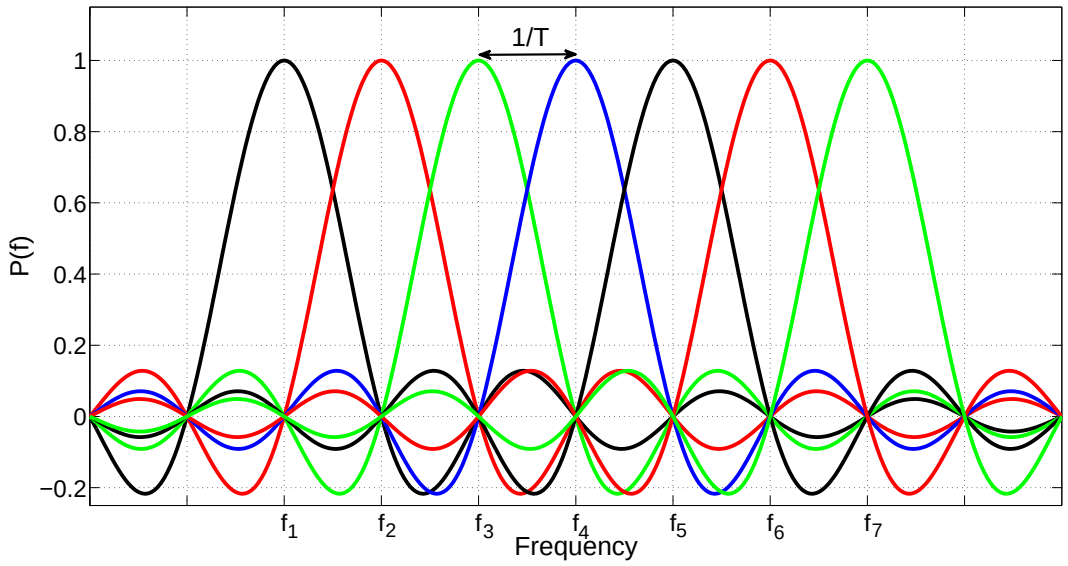

Figure 3.5: Simplified graph of an OFDM signal spectrum

3.5 Nyquist Pulse-Shaping Function

Based on the fact that each data symbol of an OFDM-based system is transmitted on a different subcarrier, the signal analysis cannot be made in the time-domain, because the envelope given by (3.1) is the result of the sum of N orthogonal signals. Therefore, it does not provide much information regarding the behavior of the digital data. The latter idea is supported by Fig. 3.4, in which we cannot ensure that subcarriers really satisfy (3.3), fact that could produce interference between them, resulting in probables information or data losses.

Alternatively, the analysis of an OFDM-based system is normally done in the frequency-domain where the measure of interference between data is given by the ICI power instead of the ISI. Graphically and in its most simplified way, the spectrum of an OFDM signal is mainly given by the Fourier transform of the pulse-shaping function $p(t)$ previously defined in Section 3.1 as $P(f)$, placed on each subcarrier frequency, as seen in Fig. 3.5. Hence, to achieve zero interference between subcarriers, $P(f)$ has to behave as a Nyquist-I pulse. This can be derived by using equations (3.1) and (3.3), leading to the following expression [14]

$$\int_{-\infty}^{\infty} p(t)\mathrm{e}^{j2\pi(f_k-f_m)t}dt = \begin{cases} 1, & \text{if } k=m \\ 0, & \text{if } k\neq m, \end{cases} \tag{3.29}$$

which indicates that $P(f)$ should have spectral null points at the frequencies $\pm 1/T, \pm 2/T, \ldots$ to ensure subcarrier orthogonality. Formally, this could be expressed as

$$P(f) = \begin{cases} 1, & \text{if } f=0 \\ 0, & \text{if } f=\pm 1/T, \pm 2/T, \ldots, \end{cases} \tag{3.30}$$

which is basically Nyquist's condition for distortionless transmission, but written in the frequency-domain.

3.5.1 Different Pulse-Shaping Functions

3.5.1.1 Rectangular Pulse (REC)

The well-known rectangular or sinc pulse introduced in Section 2.2.1, is an ideal non-causal function and, therefore, it is impossible to generate it in real systems. Although this latter fact, the sinc pulse is used in this work as a helpful benchmark or for being compared with other pulses. When referring to OFDM systems, the mathematical expression that defines the rectangular pulse behavior is given by,

$$P_{REC}(f) = \text{sinc}(fT). \tag{3.31}$$

3.5.1.2 Raised Cosine Pulse (RC)

The raised cosine function introduced in Section 2.2.1, is also useful in OFDM-based systems. But given the fact that now our problem is focused in having a sinusoidal spectrum behavior to get the most out of Nyquist's first criterion and orthogonality relationship, its time and frequency expressions given in (2.29) and (2.30), respectively, are turned around. Therefore, the raised cosine frequency-domain expression ends up being

$$P_{RC}(f) = \text{sinc}(fT)\frac{\cos(\pi\alpha fT)}{1-(2\alpha fT)^2}, \tag{3.32}$$

where α is still known as the roll-off factor and defined for every real number between 0 and 1.

At the moment, the raised cosine is one of the most (if not the most) used pulses in OFDM-based systems. The reason of its popularity is mainly because of its simple mathematical expression. This characteristic makes it an easy pulse for being implemented in digital circuits and also in software defined radios.

In this work, unless otherwise stated, the roll-off factor, α, is equal to 0.22 as suggested by the 3rd Generation Partnership Project (3GPP) for the pulse-shaping filter to be implemented at the transmitter side of the base station and UE [34,35].

3.5.1.3 'Better Than' Raised Cosine Pulse (BTRC)

The BTRC pulse aims to improve the reduction of the average ICI power caused by frequency offsets in an OFDM system. Its primary goal is to enhance the performance of the RC pulse in real OFDM-based systems, and also the one obtained by the REC pulse in ideal simulated scenarios. Its spectrum behavior is written as follows,

$$P_{BTRC}(f) = \text{sinc}(fT)\left[\frac{2\left(\frac{\pi\alpha}{\ln 2}\right)fT\sin(\pi\alpha fT)+2\cos(\pi\alpha fT)-1}{1+\left(\left(\frac{\pi\alpha}{\ln 2}\right)fT\right)^2}\right]. \tag{3.33}$$

An interesting characteristic of the BTRC pulse is that despite of the fact that the sidelobes of $P_{BTRC}(f)$ and $P_{RC}(f)$ decay as f^{-2} and f^{-3}, respectively, the BTRC still outperforms the RC in terms of ICI power because the sum given in (3.13) is completely dominated by first two sidelobes [14].

3.5.1.4 Sinc Power Pulse (SP)

The SP pulse is characterized for not depending on the roll-off factor, α. By contrast its frequency-domain expression is only given by the n-th power of the sinc function so it is simply written as,

$$P_{SP}(f) = \text{sinc}^n(fT), \tag{3.34}$$

where n is defined for every real number.

Apart from its simple mathematical expression, the SP pulse is characterized by having tails that decay faster than the ones of the REC, RC and BTRC pulses obtaining lower ICI values, but in expense of having a time-domain behavior that can poorly limit data in a optimum interval of time. In this work, unless otherwise stated, the value of the parameter n is equal to 2, because this is the one that provides the best performance of the SP pulse when implemented in OFDM-based systems [15].

3.5.1.5 Improved Sinc Power Pulse (ISP)

The ISP pulse is proposed to improve the general performance of the SP pulse by adding an extra degree of freedom to deal with the impairments shown by OFDM-based systems. Its Fourier transform is given as

$$P_{ISP}(f) = \exp\left(-a(fT)^2\right)\text{sinc}^n(fT), \tag{3.35}$$

with $\{a, n\} \in \mathbb{R}$.

Lets notice that the ISP pulse modifies the SP function by multiplying it by an exponential factor, $\exp\left(-a(fT)^2\right)$, which has a faster decaying rate for the tails of the function and thus, reduces the average ICI power better than the SP pulse [16]. In addition, as the variable a increases the central or main lobe of the pulse gets narrower, which is not a desired feature for OFDM-based systems in presence of frequency offsets because this fact increases the BER as it will be shown in Chapter 4. In this work, unless otherwise stated, the values of the parameters for the ISP are $a = 0.5$ and $n = 2$, because those are the ones proposed by the authors in [16].

3.5.1.6 New Windowing Function (NW)

The NW function is a variation of the RC pulse, but in contrast of this latter pulse it adds extra degrees of freedom and an additional exponential term to deal with technical issues

that OFDM-based systems experience. The frequency-domain mathematical expression of the NW pulse is

$$P_{NW}(f) = \exp\left(-a(fT)^2\right)\left(\operatorname{sinc}(\gamma fT)\frac{\cos\left(\pi\beta fT\right)}{1+(2\beta fT)^2}\right)^n, \tag{3.36}$$

where $\{a, \beta, \gamma, n\} \in \mathbb{R}$.

One of the main advantages that this pulse exhibits is that its sidelobes vanish faster than other pulses, therefore the ICI and SIR are minimized and maximized, respectively. Among the list of pulses under study, the NW function is also the one with the most narrow main lobe, hence the one that achieves the worst BER performance, as it will be shown later.
In this work, unless otherwise stated, the values of the parameters are $a = 2$, $n = 2$, $\beta = 1$ and $\gamma = 1$, because those are the ones proposed by the authors in [17].

3.5.1.7 Phase Modified Pulse (PM)

The PM pulse arises by trying to improve even further the ISP's ICI power reduction for an N-subcarrier OFDM-based system. Its mathematical frequency-domain expression is a generalization of the ISP pulse and it could be interpreted as a *sinc with modified phase* [18] given as,

$$P_{PM}(f) = \exp\left(-a(fT)^2\right)\left(\frac{\sin\left((\pi f - b\sin\left(c\pi f\right))T\right)}{(\pi f - b\sin\left(c\pi f\right))T}\right)^n. \tag{3.37}$$

where a, b, c and n are defined for every real number.

An special characteristic of the PM pulse is that its mathematical expression allows the sidelobes to decay at a high rate without narrowing the central lobe, hence obtaining low levels of average ICI power, high levels of average SIR power and an optimum BER curve. Moreover, it is shown in Chapter 4 that the BER curve of the PM pulse is the best one among the studied pulses.
In this work, unless otherwise stated, the values of the parameters are $a = 0.5$, $b = 0.5$, $c = 2$ and $n = 2$, because those are the ones proposed by the authors in [18].

3.6 Improve Parametric Linear Combination Pulse (IPLCP)

To define the IPLCP, which is the proposed and main pulse of this work, we first must introduce the parametric linear combination pulse (PLCP) derived in [21]. The mathematical expression of the PLCP is given by

$$P_{PLCP}(f) = \frac{\sin(\pi fT)}{\pi fT}\left(\frac{4(1-\mu)\sin^2(\pi\alpha fT/2)}{\pi^2\alpha^2(fT)^2} + \frac{\pi\alpha\mu fT\sin(\pi\alpha fT)}{\pi^2\alpha^2(fT)^2}\right), \tag{3.38}$$

where μ corresponds to the linear combination constant and it is defined for all real numbers. This constant adds an additional degree of freedom for a given roll-off factor α, which is the only independent variable in pulses like the RC or the BTRC.

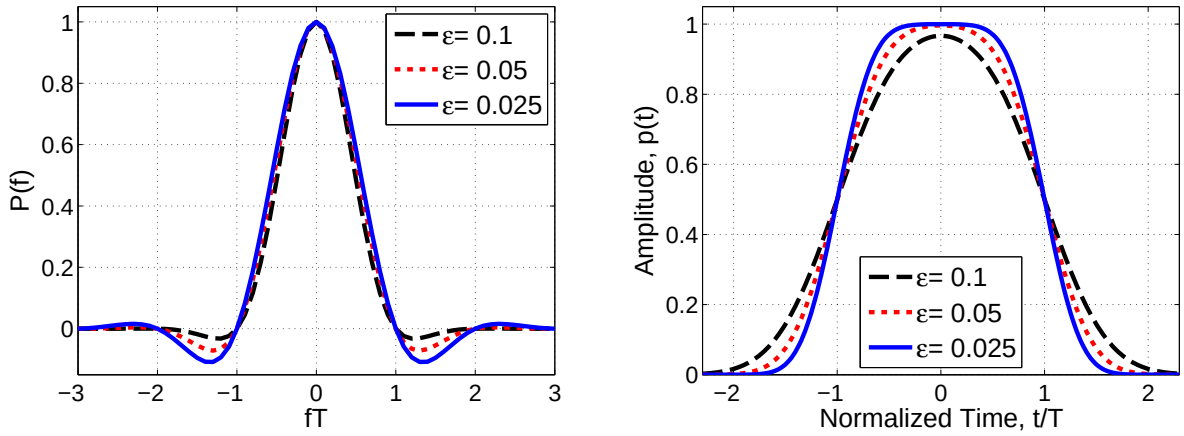

(a) (b)

Figure 3.6: (a) and (b) show the IPLCP frequency and time-domain functions, respectively, as ε varies for $\alpha = 0.22$, $\mu = 1.6$ and $\gamma = 1$.

Then, the frequency-domain expression of the IPLCP which was originally derived in [30], is given as follows

$$P_{IPLCP}(f) = \exp\left(-\varepsilon\pi^2(fT)^2\right)\left[\frac{\sin(\pi fT)}{\pi fT}\left(\frac{4(1-\mu)\sin^2(\pi\alpha fT/2)}{\pi^2\alpha^2(fT)^2} + \frac{\pi\alpha\mu fT\sin(\pi\alpha fT)}{\pi^2\alpha^2(fT)^2}\right)\right]^{\gamma}. \tag{3.39}$$

Notice that (3.39) is equivalent to the γ-th power of the PLCP multiplied by the exponential factor $\exp(-\varepsilon\pi^2(fT)^2)$. There are two extra degrees of freedom added in the frequency-domain expression of the IPLCP: γ and ε, both defined for all real numbers. It is worth mentioning that in this work, unless otherwise stated, the value of the parameter μ is set to 1.6 to be consistent with related works [21,30]. Further, to prove that the IPLCP still meets Nyquist's condition in (3.30), lets notice that (3.39) evaluated for $f = 0$ and for any value of μ, ε or γ, is always equal to one. Additionally, the IPLCP evaluated for $f = \pm 1/T, \pm 2/T, \ldots$, is always equal to zero. Therefore, the IPLCP fulfills Nyquist's first criterion.

To analyze the effects that the parameters ε and γ have on the behavior of the pulse-shaping function, only one value is varied while the other is fixed. On the one hand, as seen in Fig. 3.6(a), if the value of ε increases, the sidelobes of the IPLCP frequency function are considerably reduced without significantly affecting the central lobe width. On the other hand, it can be noticed in Fig. 3.6(b) that in the time-domain, as ε increases, the desired rectangular behavior to limit data in a precise interval of time is almost maintained. Therefore, by increasing the value of ε, an important ICI and SIR power reduction would be achieved without considerably affecting the time-domain performance, related with the ISI level of the system [30].

Further, if one fixes the value of ε and increases γ, the frequency-domain sidelobes of the IPLCP are rapidly reduced, but the central lobe width gets narrower, as seen in Fig. 3.7(a). A pulse with a narrow central lobe and almost no sidelobes (similar to a delta Dirac function) highly reduces the ICI power, but on the other hand, increases the BER of the system because the synchronization between the oscillator of the transmitter and receiver

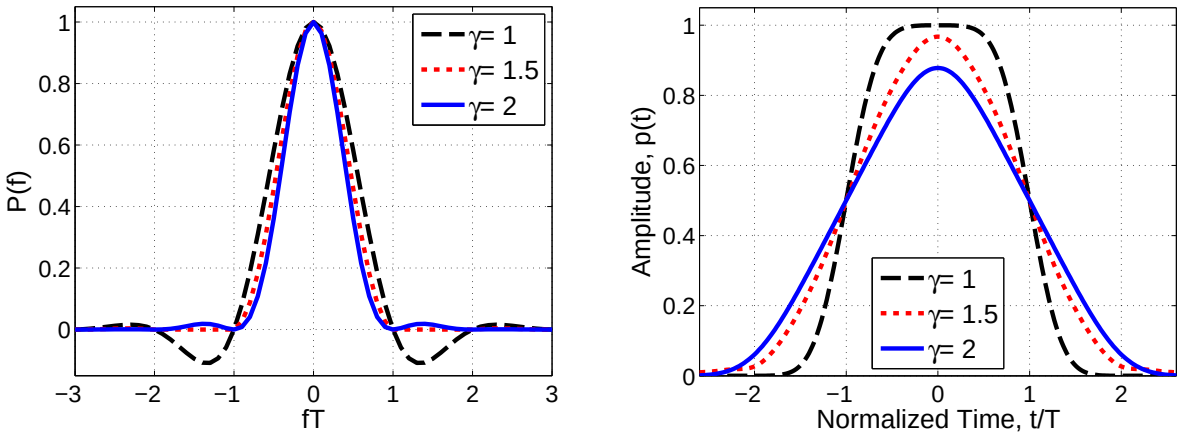

(a) (b)

Figure 3.7: (a) and (b) show the IPLCP frequency and time-domain functions, respectively, as γ varies for $\alpha = 0.22$, $\mu = 1.6$ and $\varepsilon = 0.1$.

needs to be almost perfect to recover the desired signal [16, 30], as it will be studied in the following Chapter. Furthermore, it can be seen in Fig. 3.7(b) that the time-domain behavior is not preserved as γ increases, and the IPLCP ends up looking more like a triangle function. Consequently, the pulse is not able to effectively limit the symbol duration period. Also, its amplitude is reduced attenuating the data symbols, hampering the transmission of the signal.

The frequency and time-domain responses of the IPLCP, as well as for other pulses, are illustrated in Figs. 3.8 and 3.9, respectively. As previously indicated, we fixed the value of the constant μ equal to 1.6, and through extensive computer simulations we found the

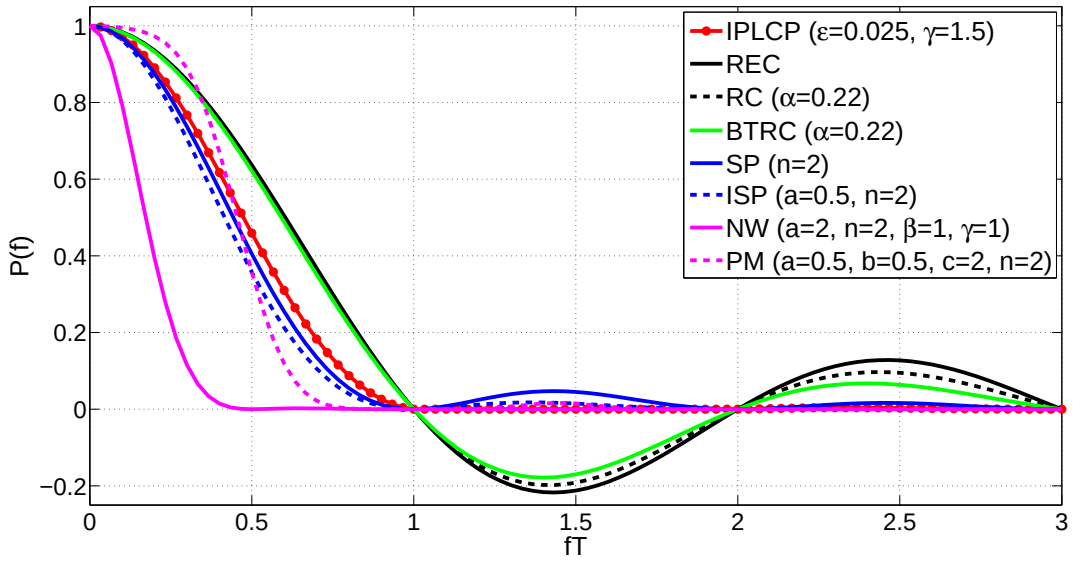

Figure 3.8: Frequency response of the IPLCP with $\mu = 1.6$ and other existing pulses.

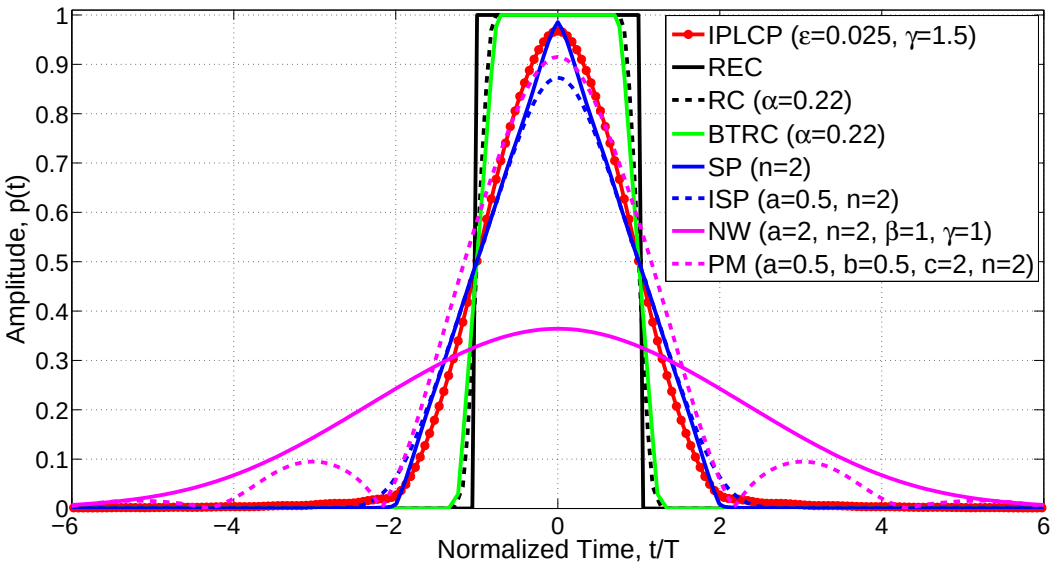

Figure 3.9: Time response of the IPLCP with $\mu = 1.6$ and other existing pulses.

sub-optimum values for ε and γ equal to 0.025 and 1.5, respectively. In general there is an optimum μ, ε, and γ for every roll-off factor and transmission scheme, although they might not be unique. The values of the parameters ε and γ were chosen taking into account the fact that the desired pulse has to have a wide central lobe and almost no sidelobes in its frequency-domain behavior, to effectively reduce the ICI (maximize the SIR) and PAPR. But also, knowing that the time-domain characteristic must be able to limit the data constellation points to avoid ISI.

From analyzing Fig. 3.8, it can be seen that the IPLCP has a similar frequency-domain response to the SP, ISP, and PM pulses. Further, the relative magnitudes of the two largest sidelobes of the previous pulses behave similarly. In order to reduce the PAPR and ICI power of the signal to be transmitted, we should design a pulse with a reduced tail size because the relative magnitudes of the two largest sidelobes are the ones that have the biggest effect on the PAPR and ICI [19, 21, 36, 37]. In the case of the NW pulse, even though its frequency response decays faster, it possesses a narrow central lobe; therefore, an increase in the average BER is expected [16, 30]. Regarding the time response of the evaluated pulses, depicted in Fig. 3.9, it can be seen that the IPLCP, SP, ISP, and PM pulses have a similar response as expected. Whereas, the time response of the NW pulse is not preserved; hence, the NW pulse is not able to effectively limit the OFDM symbol duration period and will probably increase the overall ISI obtained by the system [30]. Further, its amplitude is considerably reduced, attenuating the data symbols and increasing the BER, as shown later in this work.

3.7 Summary and Final Remarks

In this part of the work, an in-depth study of OFDM-based systems was made. At the same time, the process of generating OFDM signals was introduced and tools were given

to properly analyze such systems, which seeks to meet the requirements of orthogonality to avoid losing valuable information. Moreover, the typical problems exhibited by OFDM-based systems were presented and a complete theoretical analysis of them was made.

Subsequently, the best-know Nyquist-I pulses for implementation in OFDM system were introduced. Furthermore, the IPLCP explicit mathematical expression, which is the main pulse of this work, was derived. Regarding the latter, it was shown that the parameter ε is the one that best enhances the pulse frequency-domain behavior without considerably affecting the time-domain expression.

Finally, both frequency and time-domain behavior of each and every pulse were plotted for comparison purposes, concluding that the IPLCP behaves similarly to SP, ISP and PM. Among with the current results, it is expected to later demonstrate that the pulse under study will perform well in addressing the various problems shown by OFDM systems.

Chapter 4

Performance Evaluation of Nyquist-I Pulses in OFDM-Based Systems

In this work, we evaluate the efficiency of the IPLCP in an OFDM-based system and compare its behavior with other existing pulses, such as the REC, BTRC, SP, IS, NW and PM pulses. Theoretical and numerical simulations are shown to verify that the IPLCP outperforms the overall performance of mostly every other pulse mentioned. Optimum design parameters were used to evaluate the previous pulses, as indicated in Section 3.5. In addition, real OFDM-based systems simulated scenarios (based on the IEEE 802.11a and IEEE 802.11g WiFi protocols) were used to validate the theoretical results. Table 4.1 illustrates the parameters implemented in the simulations.

Parameter	Value
Modulation	BPSK
Number of subcarriers	64
Input data block size	52
Transmission bandwidth	20 MHz
Block oversampling	4
Signal-to-noise ratio	30 dB

Table 4.1: OFDM system simulation parameters.

4.1 ICI and SIR Performance Evaluation

To evaluate the theoretical ICI and SIR performance of the IPLCP, we can choose a certain number of subcarriers to plot (3.13) and (3.14), respectively, as the frequency offset varies. As a first approximation, we will begin by comparing the proposed pulse, for two different values of ε, only with the RC and BTRC. The reason of doing this is because the latter pulses are at the moment the most used in real communication systems applications. In Fig. 4.1 we plot both ICI and SIR expressions for the RC, BTRC and the proposed pulse for a 64 subcarrier system. It is easy to notice that the IPLCP outperforms the RC and BTRC

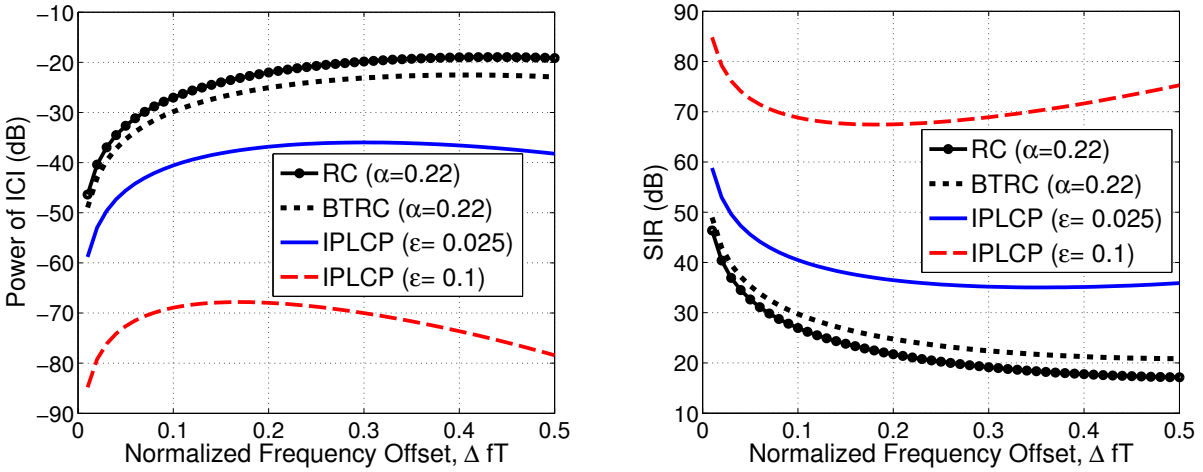

(a) (b)

Figure 4.1: (a) and (b) show the theoretical ICI and SIR power, respectively, for 64 subcarriers, $\alpha = 0.22$, $\mu = 1.6$, $\gamma = 1$ and different values of ε.

pulses in terms of ICI and SIR power for any frequency offset. In addition, Fig. 4.1 also demonstrates that increasing the value of ε improves even further the theoretical performance of the IPLCP.

Further, we evaluate the ICI power of the IPCLP and of the other pulses by simulating a 64 subcarrier OFDM-based system, using BPSK modulation and by considering the effects introduced by the channel noise. From the results shown in Fig. 4.2, it can be seen that for a normalized frequency offset higher or equal to approximately 0.15, the ICI power of the pulse-shaping functions is almost the same. For normalized frequency offsets less than 0.15, the NW pulse outperforms the other pulses, whereas the IPLCP pulse performs similarly to the SP, ISP and PM. In addition, the RC and BTRC are clearly the pulses with the worst ICI performance basically because their frequency-domain behavior have the biggest sidelobes, as previously seen in Fig. 3.8. One also may notice, that for a normalized frequency offest equal to 0.05, the NW function achieves an ICI power equal to -49 dB, whereas the IPLCP has an ICI power of -46.2 dB. Overall, as the normalized frequency offset is diminished, ICI power is reduced considerably, regardless the pulse used.

Similarly, and as it was expected given the similarities of both ICI and SIR expressions, it can be seen in Fig. 4.3 that the NW function outperforms the other pulses in terms of SIR power. Again, for small normalized frequency offsets, the NW function completely outperforms the other pulses and for larger normalized frequency offsets, the trend is almost equal for all of the pulse-shaping functions, regardless the one implemented to deal with the SIR of the system.

Furthermore, according to (3.13) and (3.14), the average ICI power of the m-th symbol depends on the number of subcarriers, and on the spectral magnitudes of the pulse-shaping function at the frequencies

$$\left(\frac{k-m}{T} + \Delta f\right), \quad k \neq m \mid k \in \{0, 1, \ldots, N\}. \tag{4.1}$$

Therefore, a pulse with small sidelobes is desired to diminish the effects of ICI and maximize the SIR power. So, in general we can conclude that the NW function outperforms the rest of the pulses in terms of ICI and SIR power because its frequency response decays faster than the other pulses, and as it was explained before, larger sidelobes will make the pulse more sensitive to both impairments, as depicted in Fig. 3.8. In addition, it can be seen from Fig. 3.8 that the NW pulse not only possesses the smallest sidelobes compared to those of the other evaluated pulses, but also the narrower central lobe. This last characteristic enables the

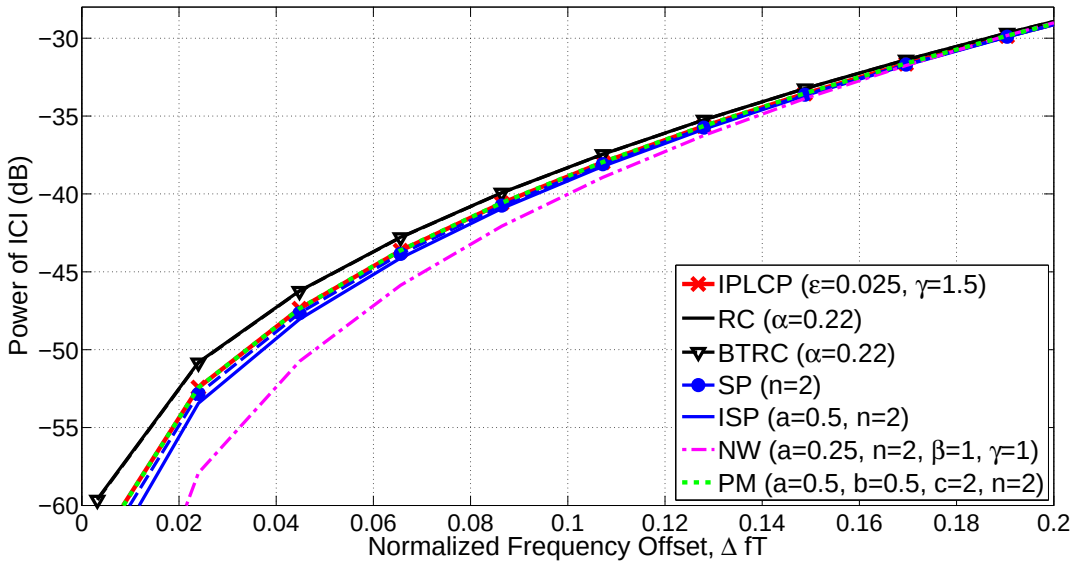

Figure 4.2: ICI power of different pulse shaping functions applied in a 64 subcarrier OFDM-based system.

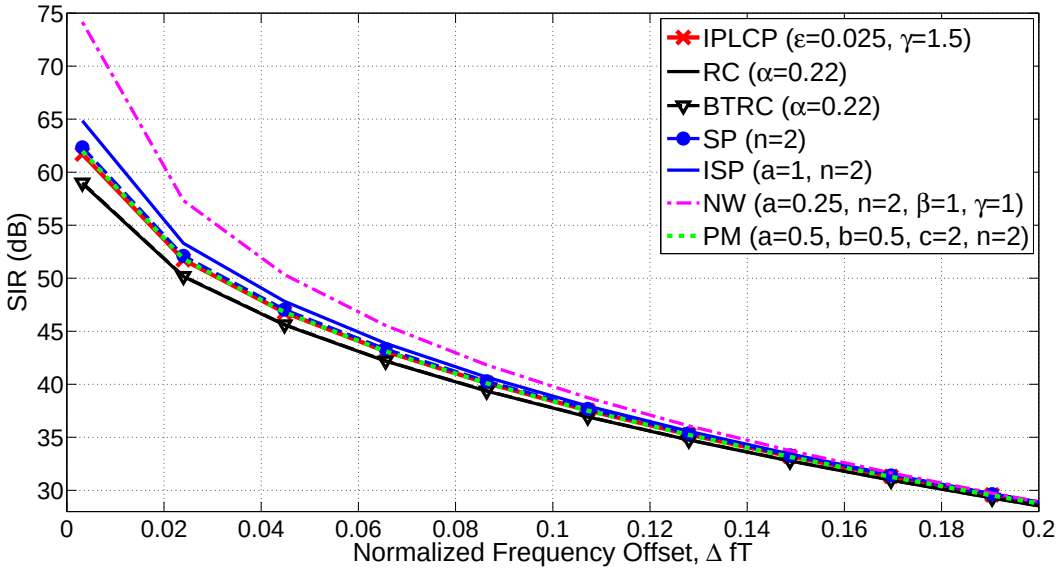

Figure 4.3: SIR power of different pulse shaping functions applied in a 64 subcarrier OFDM-based system.

pulse to practically diminish ICI between subcarriers, even though the frequency offset might reach high levels. Thinking in terms of the physical situation, a narrow central lobe generates enough space between adjacent subcarriers, so the value of Δf has to practically be equal to the minimum spacing required to satisfy orthogonality criterion $(1/T)$ for interference between subcarriers to arise.

4.1.1 PAPR Performance Evaluation

The total PAPR at the transmitter side is determined by the combination of the pulse-shaping function and the technology implemented, in this case OFDM [19,21,38]. To evaluate the PAPR of individual system configurations, we simulated the transmission of 10^5 system blocks, 64 subcarriers, and a BPSK digital modulation scheme according to the IEEE 802.11a specifications [4,39]. After calculating the PAPR of each block, the data is presented as an empirical CCDF, which measures the probability for which the transmitted signal's PAPR exceeds a certain threshold PAPR_0, $\mathbb{P}\{\text{PAPR} > \text{PAPR}_0\}$ [5,19,21]. As it was done in [19,21, 38], the PAPR was measured and analysed on the spectrum of the pulse-shaping function.

In Fig. 4.4 we plot the PAPR simulation results. It can be seen that the PM and NW are the pulses that achieves the lowest PAPR_0 among the evaluated pulses. Moreover, following the previous functions, the IPLCP, SP and ISP achieve a similar PAPR behavior. Finally, it might be argued again, that implementing pulses with smaller sidelobes further favours the performance of the OFDM-based system, but it is also worth mentioning that even though pulses like the NW perform well in terms of ICI, SIR and PAPR, the narrow central lobe characteristic that it exhibits will increase the BER of the system, as demonstrated below.

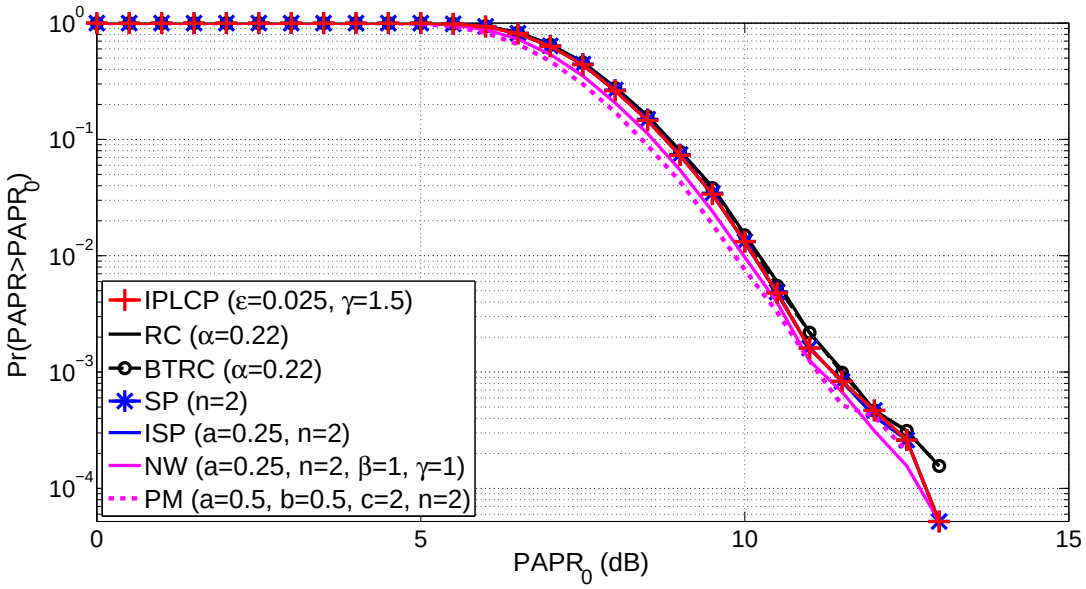

Figure 4.4: CCDF of PAPR for different pulse shaping functions applied in a 64 subcarrier OFDM-based system.

4.1.2 BER Performance Evaluation

As mentioned in Section 3.4, yielding small ICI power, maximizing SIR power, and diminishing PAPR are not the only evaluation metrics to be considered in the design of an optimal pulse-shaping function in OFDM-based systems. But, probably the most important evaluation metric in any digital communication scheme is the BER. To compare our simulation results to those obtained in [11], in this thesis we evaluate the BER of the proposed system by using a normalized frequency offset, ΔfT, equal to 0.3 and two carrier phase noises, $\theta = 10°$ and $\theta = 30°$, respectively.

In Fig. 4.5 we plot the BER of the BPSK-OFDM system with $\theta = 10°$, whereas in Fig. 4.6 we plot the BER with $\theta = 30°$. In both scenarios, the PM has the lowest BER values followed by the RC and BTRC. Further, the IPLCP is the pulse that achieves the third best BER performance in both scenarios. At this point and by analyzing the results, it may be argued that pulses with a wider central lobe achieves best BER performance than others. Moreover, by observing the pulses frequency-domain behavior in Fig. 3.8, it is possible to see that the PM is the one that has the wider main lobe, mainly because its mathematical expression in (3.37) enables it to practically diminish it tails amplitude by maintaining a broad central lobe characteristic. Continuing with this idea, the RC and BTRC also have wide central lobes, but interestingly, their sidelobes are the biggest ones among the group of pulses under study. The physical explanation of the latter thought is based on what was studied in Section 4.1, more precisely from what Fig. 4.2 shows. For values of ΔfT greater than 0.2 the system's ICI is practically the same independently of the pulse-shaping function implemented. Therefore, synchronization between local oscillators of the transmitter and receiver, ends up depending mainly on the width of the central lobe, rather than on its sidelobes amplitude. Consequently, simulation results match the expected behavior.

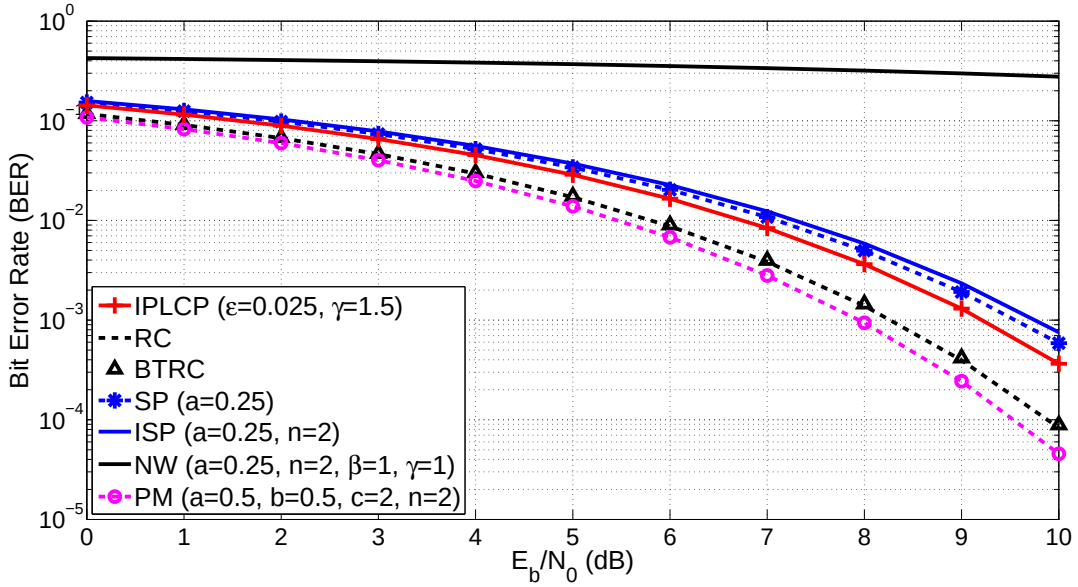

Figure 4.5: BER evaluation for different pulse shaping functions using a BPSK-OFDM system with $\Delta fT = 0.3$ and $\theta = 10°$.

Furthermore and to emphasize the above idea, the NW pulse has the worst performance among the pulses in both simulated scenarios. It may be argued that it behaves poorly because it possesses a narrow central lobe similar to a delta Dirac function, as depicted in Fig. 3.8. The latter fact increases the BER of the system due to the high synchronism that both the transmitter and receiver ends need to have to successfully recover the desired signal without errors. Moreover, it is know from literature that a lower BER is expected when the channel introduces less distortions. Then by implementing a smaller carrier phase noise angle, a better performance must be achieved. The previous statement is supported by the results shown in Figs. 4.5 and 4.6, because each pulse-shaping function obtains a lower BER curve for $\theta = 10°$, than the ones achieved when a $\theta = 30°$ value is implemented.

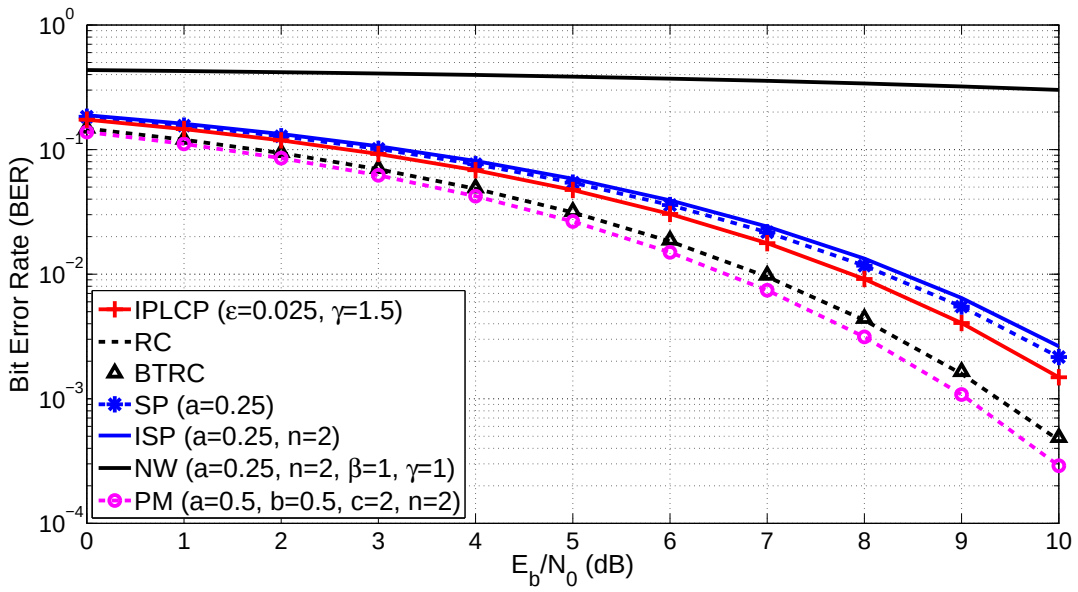

Figure 4.6: BER evaluation for different pulse shaping functions using a BPSK-OFDM system with $\Delta fT = 0.3$ and $\theta = 30°$.

4.2 Summary and Final Remarks

In this part of the thesis, the IPLCP was evaluated and compared to other well-known pulse-shaping functions in real OFDM-based systems scenarios, in terms of the ICI power, SIR power, PAPR and BER. A a roll-off factor $\alpha = 0.22$ was considered, along with the parameters that generate the best performances for each and every other pulse, based on suggestions made by the scholars that proposed them. Also, the IPLCP sub-optimum values of 0.025 and 1.5 for ε and γ, respectively, were proposed as the ones that obtain a better time and frequency-domain characteristic.

First, a simulation of the theoretical expressions of the ICI and SIR power in OFDM-based systems was introduced. For the sake of simplicity, the study was made to compare the proposed pulse with two of the most used pulses, the RC and BTRC. Simulations clearly showed that the IPLCP outperforms the recently mentioned pulses and also, that implement-

ing higher values of the parameter ε enables the system to achieve a superior performance in terms of the ICI and SIR power. Secondly, a real OFDM-based system scenario was simulated, showing that the NW pulse is the one obtaining the best ICI and SIR behavior for small frequency offset values. In addition, it was demonstrated that for values of ΔfT bigger than 0.2, the whole group of pulses performs similarly, e.g. there is less than one dB difference between the pulse-shaping functions for high ΔfT values.

Also, it was shown that the previously mentioned behavior was maintained when evaluating the performance of the system in terms of PAPR, where both NW and PM achieved the lowest values, but closely followed by the IPLCP. Further, it was shown that the NW pulse-shaping function delivers high BER curves, whereas pulses such as the IPLCP or the PM achieved low BER curves, eventually allowing the system's complexity to decrease by implementing a simpler error correction block in it.

Finally, we were able to demonstrate that the sidelobes of the pulse-shaping function implemented affects considerably the performance of the OFDM-based system in terms of the ICI, SIR and PAPR, whereas, the central lobe is the main characteristic that enhances the BER achieved by it. Therefore, obtaining pulses with no sidelobes and a wide central lobe is of top priority when designing OFDM-based systems with pulse-shaping functions implemented in it.

Chapter 5

Conclusions

In this work, Nyquist's first criterion for distortionless transmission was studied and a mathematical expression of it was derived for achieving zero interference of data in baseband communication systems. In addition, a complete study of OFDM-based systems was done, explaining which are the most common disadvantages exhibited in these systems due to channel distortions and impairments within the devices used. Also, tools where given to understand how Nyquist's condition for distortionless transmission, written in the frequency-domain, is useful when analyzing the performance of OFDM-based systems. Further, the notion of a Nyquist-I pulse-shaping function was studied and a list of the most well-known pulses was introduced. Furthermore, the recently proposed family called improved parametric linear combination pulses was analyzed, demonstrating how its main parameters, ε and γ, modify both its frequency and time-domain behavior. From the results obtained, the sub-optimum values of ε and γ were fixed to 0.025 and 1.5, and used along the whole performance evaluation process.

The IPLCP and the rest of the pulses were evaluated in terms of the ICI power, SIR power, PAPR and BER, by implementing real OFDM-based systems scenarios. Overall, the IPLCP performed well, but did not achieved the best performance for any of the evaluation metrics considered. Moreover, the NW function showed the best ICI and SIR behavior, the PM and NW pulses achieved the lowest PAPR values, and finally, the implementation of the PM pulse-shaping function minimized the BER system's performance. Therefore, it may be argued that the PM pulse is the best pulse among the list under study, but to definitely do so, one still needs to considerate its time-domain behavior, which is not as good as the one obtained by the IPLCP. The latter idea suggests that a complete ISI analysis must be done as future work to fully demonstrate the potential of the proposed pulse. The previous idea is supported by the fact that the IPLCP time-domain behavior is able to limit data points better than the SP, ISP, NW and PM. Therefore, there should exist less interference between OFDM symbols.

Hence, it is concluded that if a more complex simulation scenario (one that takes into account "timing errors" introduced by distortions within the channel, or by the devices used in the communication system) would have been implemented or, on the other hand, if the time-domain behavior of the pulses would have been considered, probably the performance

obtained by the IPLCP would be even better than the one showed in this work.

Finally, given the fact that in general there is an optimum μ, ε, and γ for every roll-off factor and transmission scheme (although they might not be unique), as future work an in-depth analysis including optimization techniques, as well as extensive computer simulations, is proposed to fully optimize the novel IPCLP pulse. And therefore, verify that it is able to completely outperform other existing pulses. In addition, it is proposed as a future work, the implementation of the IPLCP in other type of applications rather than OFDM-based systems, e.g. baseband communcation systems to reduce the ISI and BER, because its characteristics are definitely useful for these kind of schemes too.

5.1 Concluding Remarks: OFDM and 5G Networks

Similarly as it was introduced in the beginning of this work, it can be argued that the choice of the radio waveform to be implemented in the future 5G networks will have a high impact on the conception of this new technology. This is because the choice of the technology affects not only the design of transmitters and receivers, but also the complexity of the system as a whole, since each technology has different ways on addressing problems in wireless communication models. Therefore, it is essential to determine how to generate signals, determine the duration of the symbols, structure the data packets, and so on.

Given the fact that there is still no proposed standard by either the IEEE or 3GPP specifying the technical capabilities that a next generation network shall present, one can only speculate on the scopes that 5G systems will reach. Projections and stipulations of the transmission rates to be achieved in 2020 (possible release date of 5G [40]) can be seen in [41]. Now, since this type of network plans to support data transmission rates of the order of Gigabits per second (Gb/s), the waveform to be used must meet the following minimum requirements [42]:

1. Limited computational complexity for both the generation and detection.
2. Good spectrum containment [43].
3. Well-limited spectrum that enables to have small separation between the different channels assigned to each user; allowing better utilization of the total bandwidth.
4. Easily expandable to be combined with MIMO systems.
5. Deal almost perfectly with multipath transmissions.
6. Cope well with frequency selective channels.

Based on [44] and [45], it is shown that both OFDM and filter bank multicarrier (FBMC) technologies meet the above specifications better than other techniques. So at the moment they are considered as the most attractive candidates for being used in 5G networks. Going further in the results and delving a little deeper into these technologies, one may notice that the spectrum containment of FBMC responds better than OFDM, but the first is extremely much complex than the second one. On the other hand, current FBMC/MIMO models are not easy to conceive and its applicability is still not feasible for industrial levels. Whereas the

OFDM/MIMO systems already proved to be effective and enforceable in the IEEE 802.11ac protocol [46] and 4G networks. These facts makes FBMC not to respect the low complexity and easy extension to MIMO techniques that 5G networks require (items 1 and 4 of the above list). So OFDM becomes the strongest candidate for being used in the next generation systems.

Moreover, even though OFDM-based systems have gained considerable attention over the last few years, it has been noted that OFDM has to face many challenges when considered for adoption in more complex networks. Carrier and timing synchronization represent the most challenging tasks in these kind of systems [47], but another limitation of OFDM-based systems is transmitting digital data over a set of non contiguous frequency bands; also known as carrier aggregation [47]. Further, these type of systems introduce significant out of band noise to other users, as well as pick-up radiation from adjacent channels. On the other hand, FBMC is an alternative transmission method that resolves the above problems by using high quality filters that diminish out-of-band and in-band radiation [44, 47]. Additionally, FBMC systems do not need synchronization signals from the mobile nodes attached to the network [47]. Yet despite the benefits of FBMC systems, many attempts have been made to adopt the technology in various standards [47], but past and current trends seem to point to the continuity of OFDM-based systems in 5G cellular networks.

Within this work, we have successfully demonstrated the true potential of OFDM, how it deals with typical wireless communication systems channels (multipath fading channels), while it its able to achieve high data transmission rates. These latter facts, and its perfect malleability to be adapted to a wide range of functions, have allowed OFDM to be used in many past and contemporary applications. Additionally, its easy extension to MIMO systems currently allows 4G networks to considerably increase their transmission capacity and further, in a not too distant future by using massive MIMO, we will probably be able to reach transmission rates almost unthinkable for nowadays technologies [48]. Therefore, its favorable time and frequency domain characteristics makes it the clear winner for being implemented in 5G cellular networks, which would allow it to expand into the likely future heterogeneous networks (HetNets) [49] composed of macrocells, microcells, and femtocells. Meaning a significant increase in its total applications, since it could be the basis for Device-to-Device (D2D) [50], Machine-to-Machine (M2M), and Vehicle-to-Vehicle (V2V) communication protocols (IEEE 802.11p) [51].

Glossary of Acronyms and Abbreviations

1G First Generation

2G Second Generation

3G Third Generation

3GPP Third Generation Partnership Project

4G Fourth Generation

5G Fifth Generation

ADC Analog-to-Digital Converter

AWGN Additive White Gaussian Noise

BER Bit Error Rate

BPSK Binary Phase-Shift Keying

BTRC 'Better Than' Raised Cosine pulse

CCDF Complementary Cumulative Distribution Function

CDF Cumulative Distribution Function

CDMA Code Division Multiple Access

CP Ciclyc Prefix

D2D Device-to-Device

DAC Digital-to-Analog Converter

DFT Discrete Fourier Transform

DVB-T Digital Video Broadcasting - Terrestrial

EDGE Enhanced Data rates for GSM Evolution

FBMC Filter Bank Multicarriers

FDM Frequency-Division Multiplexing

GSM Global Systemm for Mobile Communications

HetNets Heterogeneous Networks

ICI Inter-Carrier Interference

IDFT Inverse Discrete Fourier Transform

IEEE Institute of Electrical and Electronics Engineers

IPLCP Improved Parametric Linear Combination pulse

ISI Inter-Symbol Interference

ISI' Institue for Scientific Information

ISP Improved Sinc Power pulse

LTE Long Term Evolution

M2M Machine-to-Machine

MIMO Multiple-Input Multiple-Output

NW New Windowing Function pulse

OFDM Orthogonal Frequency Division Multiplexing

PAPR Peak-to-Average Power Ratio

PDF Probability Density Function

PM Phase Modified Sinc pulse

PSK Phase-Shift Keying

PSTN Public Switched Telephone Network

QAM Quadrature Amplitude Modulation

RC Raised Cosine pulse

REC Rectangular pulse

SIR Signal-to-Interference Ratio

SNR Signal-to-Noise Ratio

SP Sinc Power pulse

UE User Equipment

V2V Vehicle-to-Vehicle

WCDMA Wideband Code Division Multiple Access

WiFi Wireless Fidelity

WiMAX Worldwide Interoperability for Microwave Access

WPAN Wireless Personal Area Network

Bibliography

[1] A. Pegatoquet, F. Thoen, and D. Paterson, "Virtual reality for 2.5G wireless communication modem software development," in *32nd IEEE International Computer Software and Applications*, 2008.

[2] T. Hwang, C. Yang, G. Wu, S. Li, and G. Y. Li, "OFDM and its wireless applications: a survey," *IEEE Trans. on Veh. Technol.*, vol. 58, pp. 1673–1694, May 2009.

[3] R. Nee and R. Prasad, *OFDM Wireless Multimedia Communications*. Artech House, 2000.

[4] B. H. Walke, S. Mangold, and L. Berlemann, *IEEE 802 Wireless Systems: Protocols, Multi-Hop Mesh/Relaying, Performance and Spectrum Coexistence*. Wiley, 2006.

[5] R. Prasad, *OFDM for wireless multimedia communications systems*. Artech House, 2004.

[6] H. Sari, G. Karam, and I. Jeanclaude, "Transmission techniques for digital terrestrial TV broadcasting," *IEEE Communications Magazine*, vol. 32, February 1995.

[7] W. Roh, J. Y. Seol, J. H. Park, B. H. Lee, J. K. Lee, J. S. Kim, J. Cho, K. W. Cheun, and F. Aryanfar, "Millimeter-wave beamforming as an enabling technology for 5G cellular communications: theoretical feasibility and prototype results," *IEEE Commun. Mag.*, vol. 52, pp. 106–113, Feb. 2014.

[8] T. S. Rappaport, S. Sun, R. Mayzus, H. Zhao, Y. Azar, K. Wang, G. N. Song, M. S. J. K. Schulz, and F. Gutierrez, "Millimeter wave mobile communications for 5G cellular: It will work!," *IEEE Access*, vol. 1, pp. 335–349, May 2013.

[9] S. Chen and J. Zhao, "The requirements, challenges, and technologies for 5G of terrestrial mobile telecommunication," *IEEE Commun. Mag.*, vol. 52, pp. 36–43, May 2014.

[10] R. C. Daniels, J. N. Murdock, T. S. Rappaport, and R. W. Heath, "60 GHz Wireless: up close and personal," *IEEE Microwave Magazine*, vol. 11, pp. 44–50, Dec. 2010.

[11] K. N. Le, "Insights on ICI and its effects on performance of OFDM systems," *Digital Signal Processing*, vol. 18, pp. 876–884, Nov. 2008.

[12] P. Tan and N. Beaulieu, "Analysis of the effects of Nyquist pulse-shaping on the performance of OFDM systems with carrier frequency offset," *European Trans. on Telecom-*

munications, vol. 20, pp. 9–22, July 2009.

[13] S. Mohanty and S. Das, "A comparative study of pulse shaping functions for ICI power reduction in OFDM system," in *Annual IEEE India Conference*, pp. 312–316, IEEE, Dec. 2008.

[14] N. C. Beaulieu and P. Tan, "Reduced ICI in OFDM systems using the "better than" raised-cosine pulse," *IEEE Commun. Lett.*, vol. 8, pp. 135–137, Mar. 2004.

[15] H. M. Mourad, "Reducing ICI in OFDM systems using a proposed pulse shape," *Wireless Pers. Commun*, vol. 40, pp. 41–48, Jan. 2006.

[16] V. Kumbasar and O. Kucur, "ICI reduction in OFDM systems by using improved sinc power pulse," *Digital Signal Processing*, vol. 17, pp. 997–1006, Apr. 2007.

[17] P. K. Yadav, V. K. Dwivedi, V. Karwal, and J. P. Gupta, "A new windowing function to reduce ICI in OFDM systems," *International Journal of Electronics Letters*, vol. 2, no. 1, pp. 2–7, 2014.

[18] N. D. Alexandru and A. L. Onofrei, "ICI reduction in OFDM systems using phase modified sinc pulse," *Wireless Pers. Commun*, vol. 53, pp. 141–151, Mar. 2010.

[19] C. A. Azurdia-Meza, K. J. Lee, and K. S. Lee, "PAPR reduction by pulse shaping using Nyquist linear combination pulses," *IEICE Electronics Express*, vol. 9, pp. 1534–1541, Oct. 2012.

[20] J. Choi, K. Kang, K. Kim, J. Park, B. Jin, and B. Kim, "Power amplifiers and transmitters for next generation mobile headsets," *Journal of Semiconductor Technology and Science*, vol. 9, pp. 249–256, Dec. 2009.

[21] C. A. Azurdia-Meza, K. Lee, and K. Lee, "PAPR reduction in SC-FDMA by pulse shaping using parametric linear combination pulses," *IEEE Communications Letters*, vol. 16, pp. 2008–2011, Dec. 2012.

[22] H. G. Myung, J. Lim, and D. J. Goodman, "Single carrier FDMA for uplink wireless transmission," *IEEE Vehicular Technology Magazine*, vol. 1, pp. 30–38, Sept. 2006.

[23] H. G. Myung, J. Lim, and D. Goodman, "Peak-to-average power ratio of single carrier FDMA with pulse shaping," in *IEEE 17th International Symposium PIMRC*, 2006.

[24] B. Berglund, J. Johansson, and T. Lejon, "High efficiency power amplifiers," *Ericson Review*, vol. 83, no. 3, pp. 92–96, 2006.

[25] H. Nyquist, "Certain Topics in Telegraph Transmission Theory," *Transactions of the American Institute of Electrical Engineers*, 1928.

[26] J. G. Proakis and M. Salehi, *Digital Communications*. McGraw-Hill, 2007.

[27] N. Beaulieu, "Introduction to Certain Topics in Telegraph Transmission Theory," *Pro-*

ceedings of the IEEE, vol. 90, February 2002.

[28] N. Sheikholeslami and P. Kabal, "Generalized raised-cosine filter," *IEEE Transactions on Communication*, vol. 47, July 1999.

[29] S. B. Weinstein, "The history of Orthogonal Frequency-Division Multiplexing," *IEEE Commun. Mag*, vol. 47, pp. 26–35, November 2009.

[30] H. F. Arraño and C. A. Azurdia-Meza, "ICI reduction in OFDM systems using a new family of Nyquist-I pulses," in *IEEE Latin-America Conference on Communications*, 2014.

[31] P. Tan and N. Beaulieu, "A novel pulse-shaping for reduced ICI in OFDM systems," in *IEEE 60th. Vehicular Technology Conference*, vol. 1, pp. 456–459, 2004.

[32] D. D. Wackerly, W. Mendenhall, and R. L. Scheaffer, *Mathematical Statistics with Applications*. Thomson Books/Cole, 7 ed., 2008.

[33] A. Goldsmith, *Wireless Communications*. Cambridge University Press, 2005.

[34] Third Generation Partnership Project (3GPP), "Universal Mobile Telecommunications System (UMTS); Base station BS radio transmission and reception FDD," Tech. Rep. 125.104, European Telecommunications Standards Institute, 2014.

[35] 3rd Generation Partnership Project (3GPP), "Universal Mobile Telecommunications System (UMTS); User equipment UE radio transmission and reception FDD," Tech. Rep. 125.101, European Telecommunications Standards Institute, 2014.

[36] B. Farhang-Boroujeny, "A square-root Nyquist M filter design for digital communication systems," *IEEE Trans. Signal Process.*, vol. 56, pp. 2127–2132, May 2008.

[37] B. Chatelain and F. Gagnon, "Peak-to-average power ratio and intersymbol interference reduction by Nyquist optimization," in *IEEE Vehicular Technology Conference*, 2004.

[38] Y. D. Wei and Y. F. Chen, "Peak-to-average power ratio PAPR reduction by pulse shaping using the K-exponential filter," *IEICE Trans. Commun.*, vol. E93-B, pp. 3180–3183, Nov. 2010.

[39] *IEEE wireless LAN edition - a compilation based on IEEE Std. 802.11TM-199 (R2003) and its amendments*. IEEE Standard, R2003.

[40] W. Roh, J. Y. Seol, J. H. Park, B. H. Lee, J. K. Lee, J. S. Kim, J. Cho, K. W. Cheun, and F. Aryanfar, "Milimeter-wave beamforming as an enabling technology for 5G cellular communications: theoretical feasibility and prototype results," *IEEE Commun. Mag.*, vol. 52, pp. 106–113, Feb. 2014.

[41] G. Fettwels and S. Alamouti, "5G: personal mobile internet beyond what cellular did to telephony," *IEEE Communication Magazine*, vol. 52, pp. 140–145, February 2014.

[42] G. Berardinelli, K. Pajukoski, E. Lahetkangas, R. Wichmann, O. Tirkkonen, and P. Mogensen, "On the Potential of OFDM Enhancements as 5G Waveforms," in *IEEE Vehicular Technology Conference*, pp. 1–5, May 2014.

[43] S. C. Thompson, A. U. Ahmedt, J. G. Proakis, and J. R. Zeidler, "Constant envelope ofdm phase modulation: Spectral containment, signal space properties and performance," in *IEEE Military Communications Conference*, vol. 2, pp. 1129–1135, October 2004.

[44] B. Farhang-Boroujeny, "OFDM versus filter bank multicarrier," *IEEE Signal Processing Magazine*, vol. 28, pp. 92–112, May 2011.

[45] F. Schaich, "Filterbank based multi carrier transmission (FBMC)-evolving OFDM," in *European Wireless Conference*, pp. 1051–1058, April 2010.

[46] R. P. F. Hoefel, "Multi-user OFDM MIMO in IEEE 802.11ac WLAN: A simulation framework to analysis and synthesis," in *IEEE Latin-America Conference on Communications*, November 2013.

[47] B. Farhang-Boroujeny, "Filter bank multicarrier modulation: a waveform candidate for 5G and beyond," *Advances in Electrical Engineering*, vol. 2014, pp. 1–25, December 2014.

[48] E. G. Larsson, O. Edfors, F. Tufvesson, and T. L. Marzetta, "Massive MIMO for next generation wireless systems," *IEEE Communications Magazine*, vol. 52, pp. 186–195, February 2014.

[49] N. Bhushan, J. Li, D. Mallad, R. Gilmore, D. Breneer, A. Damnjanovic, R. T. Sukhavasi, C. Patel, and S. Geirhofer, "Network densification: the dominant theme for wireless evolution into 5G," *IEEE Communications Magazine*, vol. 52, pp. 82–89, February 2014.

[50] B. Banderte, S. Talwar, R. Arefi, and K. Stewart, "Networks and devices for the 5G era," *IEEE Communications Magazine*, vol. 52, pp. 90–96, February 2014.

[51] *Local and metropolitan area networks, Specific requirements. Part 11: Wireless LAN Medium Access Control (MAC) and Physical Layer (PHY) Specifications Amendment 6: Wireless Access in Vehicular Environments.* IEEE Standard for Information Technology, 2010.

Appendix A: List of Publications

Institue for Scientific Information (ISI') Journals

1. Hernán F. Arraño, Cesar Azurdia-Meza, "ICI Reduction in OFDM Systems Using a New Family of Nyquist-I Pulses", accepted in *IEEE Latin America Transactions*, April 2015.
2. Cesar Azurdia-Meza, Hernán F. Arraño, Claudio Estevez and Ismael Soto, "Performance Enhancement of OFDM-Based System using Improved Parametric Linear Combination Pulses", *Wireless Personal Communications*, June 2015. DOI 10.1007/s11277-015-2810-7

Conference Publications

1. Hernán F. Arraño, Cesar Azurdia-Meza, "ICI Reduction in OFDM Systems Using a New Family of Nyquist-I Pulses", in *6th IEEE Latin-American Conference on Communications*, November 2014, Cartagena de Indias, Colombia.
2. Hernán F. Arraño, Cesar Azurdia-Meza, "OFDM: Hoy y en el Futuro de las Comunicaciones", in *XV Congreso Internacional de Telecomunicaciones*, November 2014, Valdivia, Chile.
3. Hernán F. Arraño, Cesar Azurdia-Meza, "Pulsos de Nyquist para la Reducción del ICI en Sistemas OFDM", in *XV Congreso Internacional de Telecomunicaciones*, November 2014, Valdivia, Chile.

Submitted Articles

1. Hernán F. Arraño, Cesar Azurdia-Meza, Kyesan Lee, "OFDM: Today and in the Future of Next Generation Wireless Communications", submitted to *7th IEEE Latin-American Conference on Communications*, July 2015.
2. Cesar Azurdia-Meza, Angelo Falchetti, Hernán F. Arraño, S. Kamal and Kyesan Lee, "Evaluation of the Improved Parametric Linear Combination Pulse in Digital Baseband Communication Systems", submitted to *International Conference on Information and Communication Technology Convergence*, July 2015.